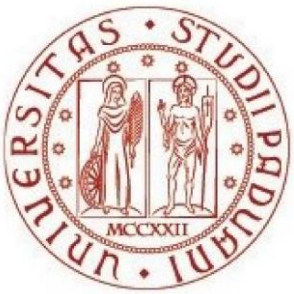

UNIVERSITÀ DEGLI STUDI DI PADOVA

DEPARTMENT OF ENGINEERING

MASTER'S DEGREE IN "ICT FOR INTERNET AND MULTIMEDIA"

FINAL DISSERTATION

PIPELINE FOR QUALITATIVE ANALYSIS OF DATA TRANSMISSION FROM IOT NETWORK'S-LoRaWAN IN AN URBAN ENVIRONMENT

SUPERVISOR: ***LEONARDO BADIA***

STUDENT: VENKATA RAJESH CHINTA

STUDENT ID: 2005632

ACADEMIC YEAR- 2023-2024

ABSTRACT

This research endeavor has dual objectives: firstly, it involves the collection of environmental data, including air quality measurements, and secondly, it evaluates the efficiency of LoRaWAN sensor-based solutions in transmitting data over long distances across open seas and outdoor environments. This initiative aligns with the deployment of a LoRaWAN infrastructure, jointly developed by the same collaborating partners, at the CNR headquarters in Genova towards the conclusion of the summer. This initial setup included one gateway and one air quality monitoring station.

The subsequent phase, which is already in the planning stages, encompasses the establishment of a second LoRaWAN-based air quality monitoring station at the CNR pier within the city's harbor area. The primary objective is to gather environmental data and assess the performance of the employed sensing and communication technologies.

For at least a decade, Gruppo SIGLA and CNR-IAS have maintained a collaborative partnership, actively engaging in various initiatives aimed at incorporating cutting-edge IT features for the monitoring of maritime regions and vital environmental factors in this domain. Their recent involvement in projects funded by the Liguria Region, namely PICKUP and TIAMO, underscores their ongoing commitment to advancing these endeavors.

ACKNOWLEDGEMENT

Firstly, I would like to thank the University Degli Studi di Padova and the ICT for Internet and Multimedia for the opportunities that was offered to me.

I would like to express my sincere gratitude to all those who have supported me throughout the course of my research and the writing of this thesis.

First and foremost, I would like to thank my thesis coordinator, **"LEONARDO BADIA",** for his invaluable guidance, encouragement, and support throughout my internship at **"GRUPPO SIGLA"**. His insights and expertise were instrumental in shaping my research and helping me achieve my goals.

I would also like to express my heartfelt thanks to the team at "Gruppo Sigla," who provided me with an opportunity to work on a challenging and rewarding project and supported me with their expertise and resources.

Finally, I would like to acknowledge the love and support of my family and friends, whose unwavering encouragement and belief in me have been a source of strength throughout my academic journey.

Thank you all for your invaluable contributions to my research and my personal growth.

Table of Contents

List of Figures:

List of Tables:

CHAPTER-1

1. INTRODUCTION:

The paradigm of the Internet of Things (IoT) converges diverse information, establishing a communication framework for devices and applications. This process initiates as devices securely connect to an IoT platform, [6] which serves as a hub for integrating data from numerous devices. Through analytics, this platform disseminates the most valuable information to applications tailored to address industry-specific needs. Equipped with hardware, sensors, and actuators, these devices can autonomously exchange information over a network, eliminating the need for direct human-to-human or human-to-computer communication. IoT applications necessitate specific attributes such as reliability, performance, quality, and long-term availability [1].

1.1LPWAN of IoT:

Based on their operating range, LPWAN systems can be roughly divided into two categories: licensed and license-free. [3] While the 3GPP cellular standards constitute the root of all licensed spectrum LPWANs, the license-free market is significantly more varied [2]. These solutions are centered on the Ultra-Narrowband, Spread Spectrum, and Telegram Splitting technologies.

Low power wide area network (LPWAN) technology provides the low-cost, low power, and wide-area coverage needed for robust IoT sensor networks to secure data transportation. Figure 1 depicts the comparison of LPWAN technologies.

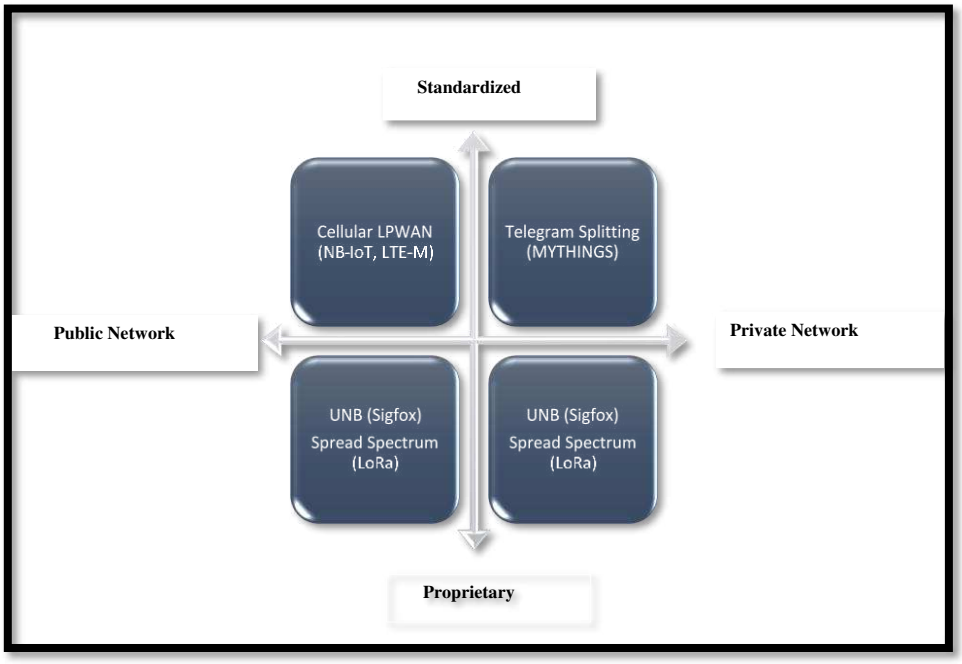

Figure 1: Comparison of LPWAN technologies [Web 1].

There are four main LPWAN technologies available on the market that can be divided into licensed and license-free categories based on their operational spectrum:

Cellular LPWAN: This technology leverages the licensed spectrum and the existing cellular infrastructure for data transmission, benefiting from minimal co-channel interference, thus ensuring dependable data transfer. However, this operation necessitates more intricate protocols, as the nodes must first secure approval from the base station to transmit a message; achieving this authorization may require multiple attempts, potentially resulting in a notable increase in power consumption.

Traditional Ultra Narrowband: This technology utilizes an exceptionally narrow bandwidth for information transmission, showcasing outstanding spectrum efficiency. Its low data rate enables receivers to detect and decode signals at extended

distances, expanding the coverage range. On the flip side, this elongates the transmission duration, [81] consequently escalating power consumption and rendering the system more vulnerable to interference from other devices operating within the same frequency range [3][4].

Spread Spectrum: This technique employs coding to surmount a high noise floor, elevating receiver sensitivity and enabling long-range transmission of a minute signal across a broad frequency band, thereby making it challenging to detect and intercept. However, [81] there is a significant risk of self-interference when a narrowband signal is spread over a wideband channel, diminishing network capacity [3][4].

Telegram Splitting: This method dissects an ultra-narrowband signal into numerous smaller sub-packets, subsequently broadcasting these sub-packets as brief radio bursts at various frequencies and time intervals. To minimize collision potential with other sub-packets, it employs short airtime and pseudo-randomness. This approach enhances both robustness and scalability while reducing interference [7].

1.2 LoRaWAN ARCHITECTURE:

LoRa: Proprietary radio modulation to connect between end devices and gateways.

LoRaWAN:

The LoRaWAN Network Server and the end device communicate via an access control protocol that operates at the MAC layer (MAC-media access control). A physical layer technology called LoRa uses a customized form of spread spectrum to modulate communications in the sub-GHz ISM band. LoRa utilizes unlicensed ISM bands, just like Sigfox. A chirp spread spectrum (CSS) modulation, which spreads a narrowband signal over a broader channel bandwidth, is used to provide the communication [8].

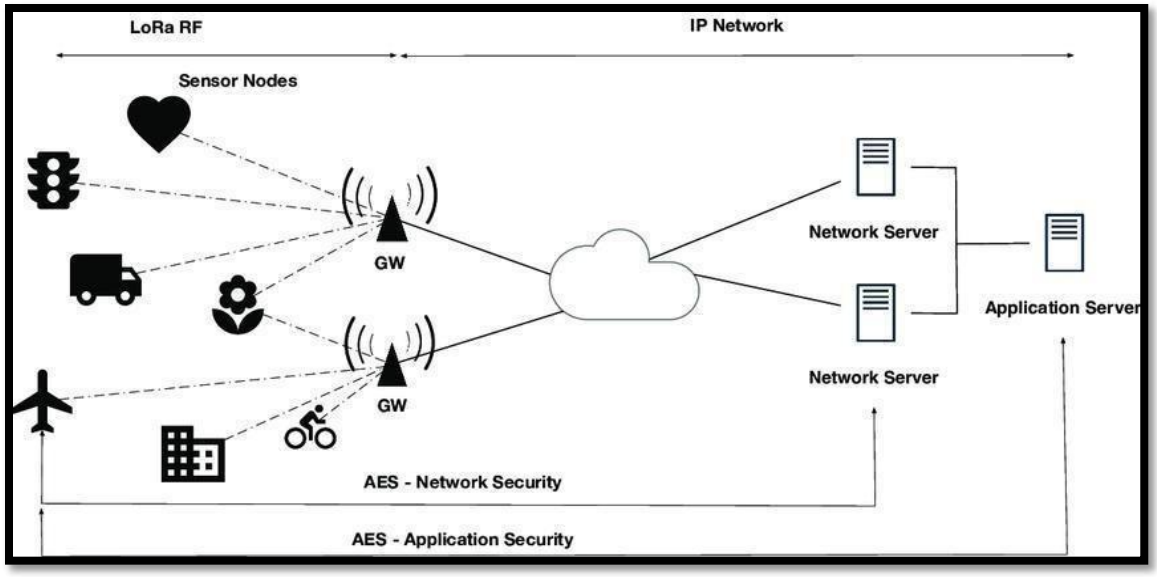

Figure 2: illustrates the Architecture of LoRaWAN Network [8].

1.3 SIGFOX:

A provider of LPWAN networks, Sigfox provides a complete IoT connection solution underpinned by its unique technologies. Sigfox installs it is own base stations, which come with cognitive software-defined radios, and uses an IP-based network to link them to the backend servers. Sigfox employs unlicensed ISM bands, such as 433 MHz in Asia, 868 MHz in Europe, and 915 MHz in North America. There is a limit of 140 messages per day that can be sent over the uplink. Each uplink message can have a payload as long as 12 bytes. The fact that the downlink can only send a maximum of four messages per day suggests that the acknowledgment of each uplink message is unsupported [10].

1.4 LoRaWAN TECHNOLOGY:

As depicted in the diagram, Lora's network exhibits characteristics of "a star-of-star topology." A LoRa network is made up of several elements: [10] [11] [12]

1. Endpoints:

Endpoints are low-cost, battery-powered gadgets. [6] They are elements of the LoRa network that do sensing or controlling. Most of the time, they are far away.

2. The LoRa Gateway:

Collects communications from LoRa endpoints and routes them to the backhaul network. This component of the LoRa network could be cellular, Ethernet, or any other type of telecommunication's connectivity. Standard IP connections are used to connect the gateways and the network server.

3. The LoRa Network Server (NS):

The center of the star-shaped topology is where the LoRa Network Server (NS) is situated. The management and connection of LoRa end devices, gateways, and end-user applications is the responsibility of LoRaWAN network servers. Additionally, they ensure that data being sent to the network is secure. The universal properties of NS are:

(a) End-Device address check

(b) Data rate adaptation

(c) Responding to MAC layer requests sent by the end device.

(d) Forwarding uplink application payloads to the specific Application Servers

(e) Queuing of downlink payloads coming from any Application Server to any End Device connected to the network.

(f) Forwarding Join-request and Join-accept messages between the End-Devices and the Join Servers.

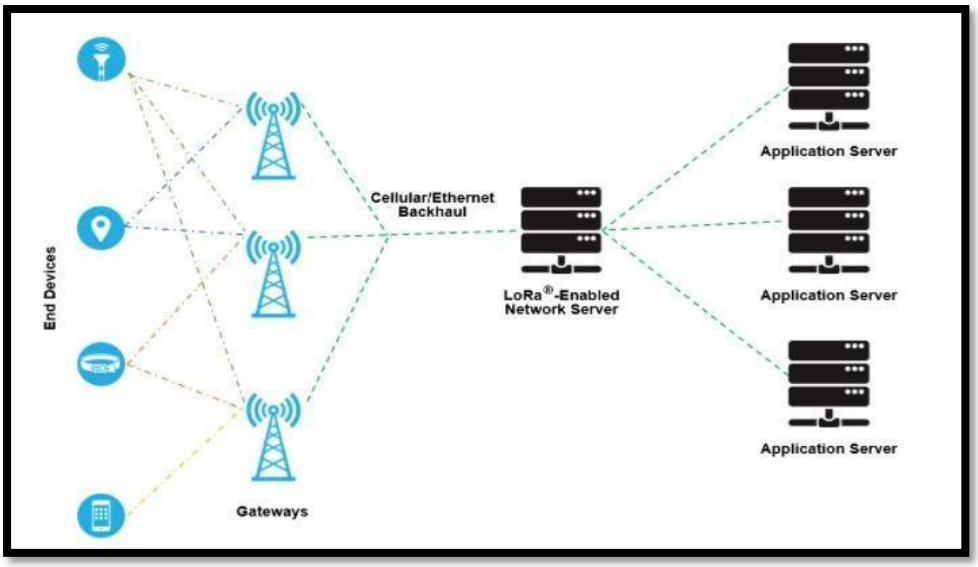

Figure 3: Sketch of LoRaWAN Network[10].

CHAPTER-2

2.1 LoRaWAN CLASSES:

The [45] LoRaWAN framework encompasses Class A, Class B, and Class C devices. Class A and Class B end devices are commonly battery-powered, while Class C end devices typically rely on a mains power source. When it comes to energy efficiency, Class A outperforms both Class B and Class C [13].

Class A end devices transmit confirmed messages during two predetermined time intervals referred to as "Receive Windows (RW)" and subsequently await acknowledgment (ACK) from the Network server. Figures: 4, 6 &7 illustrate the RWs for Class A, Class B, and Class C operating modes. The first RW operates at the same frequency and data rate as the uplink transmission parameters, while the second RW follows established guidelines. Unconfirmed communications do not elicit responses from end devices.

Gateways have the capability to schedule additional receive windows using Class B operating mode and beacon packets, requiring periodic beacons from the gateway for synchronization. In contrast, Class C mode consumes significantly more energy as it imposes no downlink restrictions and is always ready to receive downlink messages when not actively transmitting.

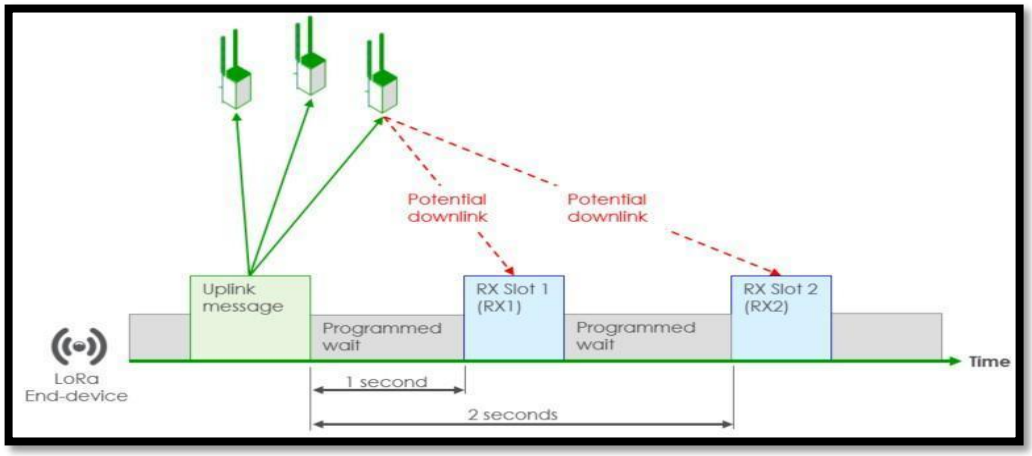

Figure 4: LoRaWAN Class -A transmit / receive [14]

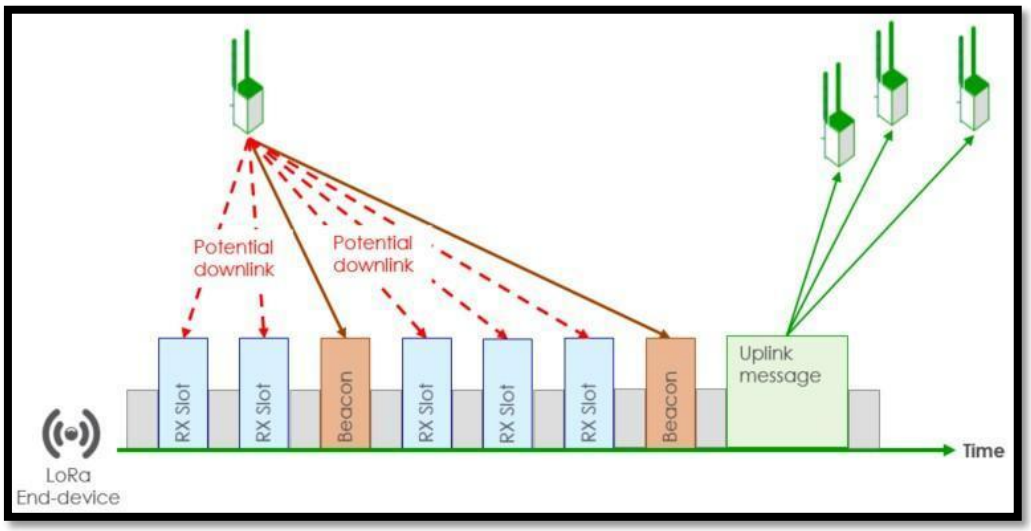

Figure 5: LoRaWAN Class-B transmit/receive [14]

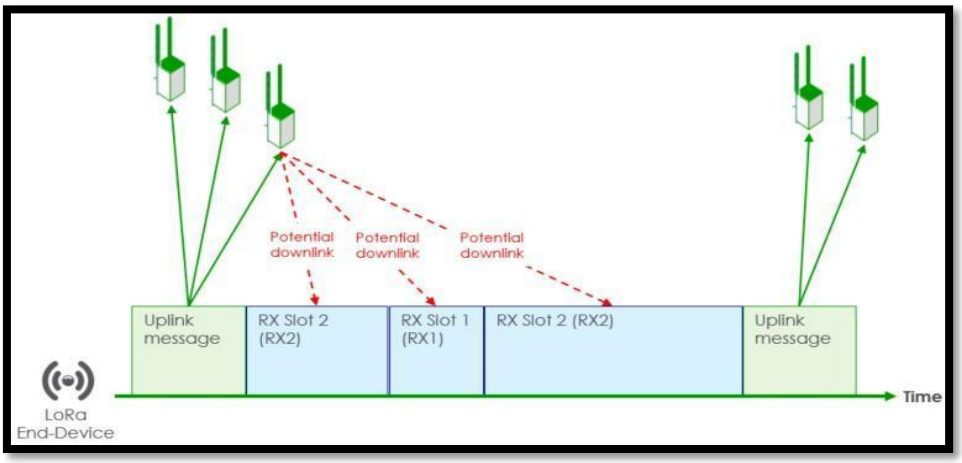

Figure 6: LoRaWAN Class-C transmit/receive [14]

LoRaWAN does not provide inter-device communication. Packets can only be sent from an end device to a gateway or vice versa. Figure depicts the LoRaWAN protocol stack. The physical layer defines the ISM bands, while the LoRa modulation layer is appropriate for long-distance communication with low power consumption. Semtech has used CSS modulation to do this [15].

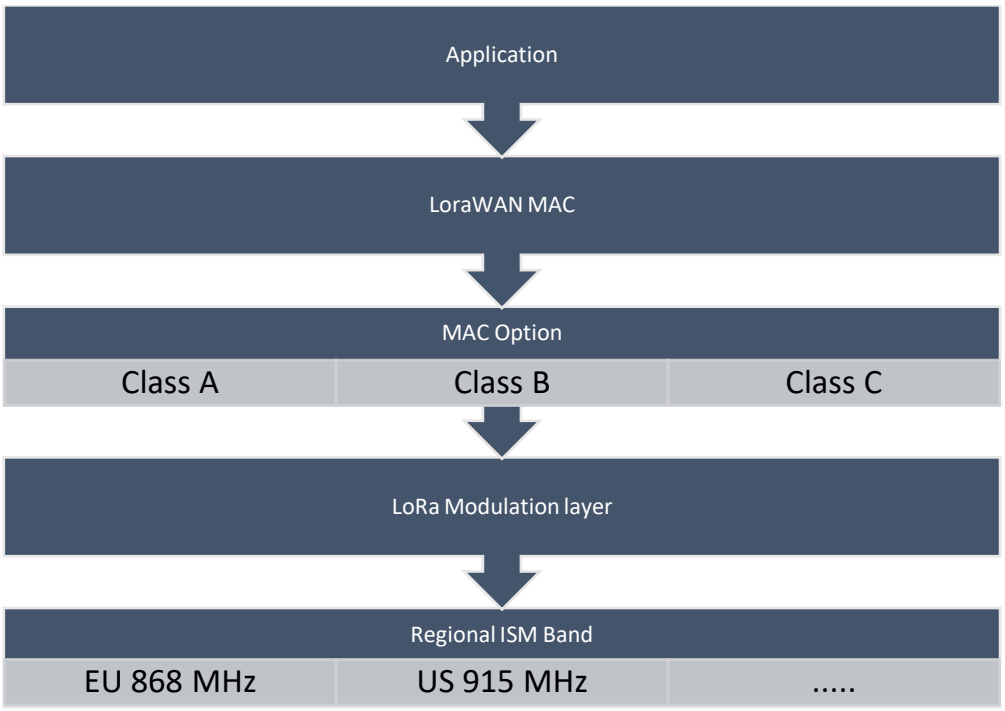

Figure 7: LoRaWAN PROTOCOL STACK[15].

2.2 LoRaWAN Power Consumption:

The power consumption of LoRaWAN devices can vary depending on several factors, including the specific hardware used, the operating mode (Class A, Class B, or Class C), the duty cycle regulations in the region, and the frequency of data transmissions. Here is a general overview of power consumption considerations for LoRaWAN devices:

CLASS A, B, OR C MODE: The LoRaWAN specification defines three classes of end devices, each with different power consumption characteristics. Class A devices are the most power efficient as they have specific receive windows after transmitting data. Class B devices have scheduled receive windows, and Class C devices have continuous receive windows. Class C devices typically consume more power than Class A and B devices due to their constant listening.

Transmit Power: The transmit power level used by the device can significantly impact power consumption. Higher transmit power typically requires more energy.

DATA RATE: The LoRa modulation used by LoRaWAN allows for various data rates. Lower data rates generally result in longer range but may also consume more power, especially during transmission.

DUTY CYCLE REGULATIONS: Regulatory authorities in different regions often impose duty cycle restrictions, limiting the amount of time a device can transmit data. Adhering to these regulations is essential to avoid excessive power consumption and interference with other devices.

SLEEP MODES: Many LoRaWAN devices have sleep modes where they consume minimal power when not actively transmitting or receiving data. Properly configured sleep modes can extend battery life.

BATTERY TYPE: The type and capacity of the battery used in the device play a crucial role in determining how long the device can operate before requiring a battery replacement or recharge.

DATA TRANSMISSION FREQUENCY: How often the device needs to send data impacts its power consumption. Infrequent transmissions allow for longer battery life.

ENVIRONMENTAL CONDITIONS: Temperature and other environmental factors can influence the efficiency of the device and, consequently, its power consumption. To accurately assess the power consumption of a specific LoRaWAN device, it is essential to refer to the device is datasheet and consider the factors mentioned above. Additionally, conducting power consumption tests in the target deployment environment can provide valuable insights into real-world power usage.

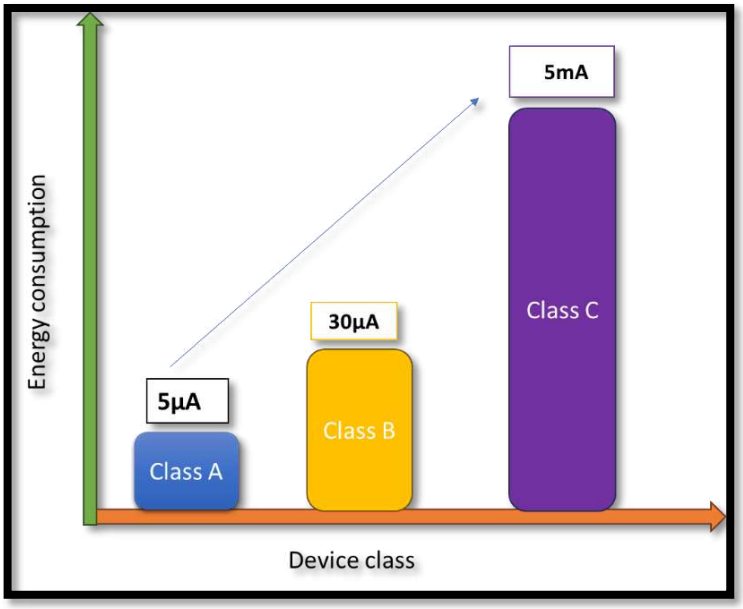

Figure 8: Energy Consumption by Device Class [16].

2.3 LoRaWAN (MAC Layer):

The data-link protocol LoRaWAN controls how LoRa devices connect to the network and how they exchange data, as well as the addresses they use, the encryption used, and other packet parameters. While LoRa might be likened to Ethernet (as a physical layer), LoRaWAN could be compared to the IP protocol.

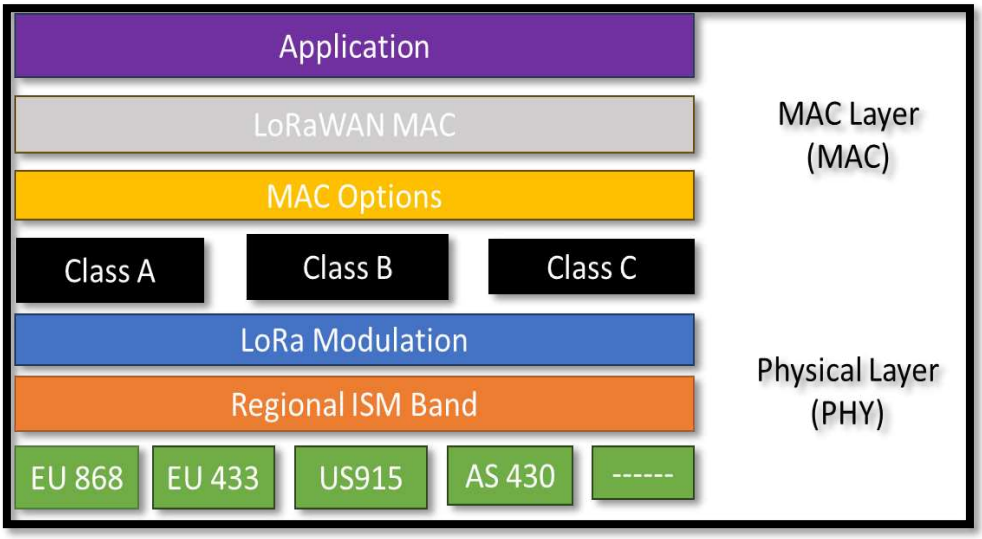

Figure 9: LoRa AND LoRaWAN ON THE OSI MODEL [17].

2.3.1 MAC Message Formats:

LoRaWAN MAC messages are contained within the radio PHY payload of the Lora protocol. The structure of a PHY payload is illustrated in figure. Furthermore, the MAC payload field can alternatively be exchanged for a network join request or a join-response, if necessary. We will not expand further on the network join-requests and responses in this thesis. The MAC header (MHDR) and message.

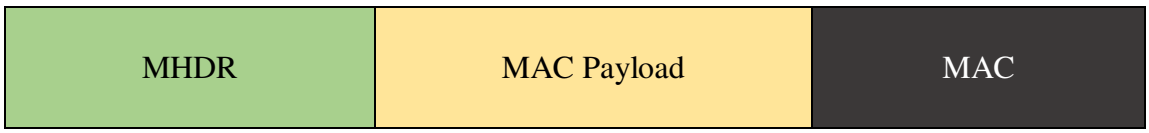

Figure 10: MAC Message Formats

2.3.2 PHY Message Formats:

LoRa the radio protocol utilizes the PHY headers to make radio-transmission and reception possible. There exists two PHY formats, one for up-link and one for down-link messages. The difference between those formats is that the up-link format contains an optional cyclic redundancy check (CRC) field. The PHY uplink message format is structured as can be seen in figure.

Figure 11: PHY Message Formats

1. LoRa Devices (End Devices):

They are electronic IoT embedded systems with low power requirements, compact designs, and affordable prices. These devices must have a LoRa Radio in order to transmit using LoRa protocols.

2. LoRa Gateway:

They are technological gadgets with the capacity to simultaneously listen on several channels and on all spreading factors. Once they have a LoRa frame, they transfer the content of the frame to the web server through the internet. It acts as a conduit for both LoRa modulation and IP transmission. Each LoRa Gateway has its own unique identification (64-bit EUI). This identity is useful for setting up a network server, including establishing a gateway (more on that in subsequent chapters). A LoRa frame follows the steps depicted in Figure 12.

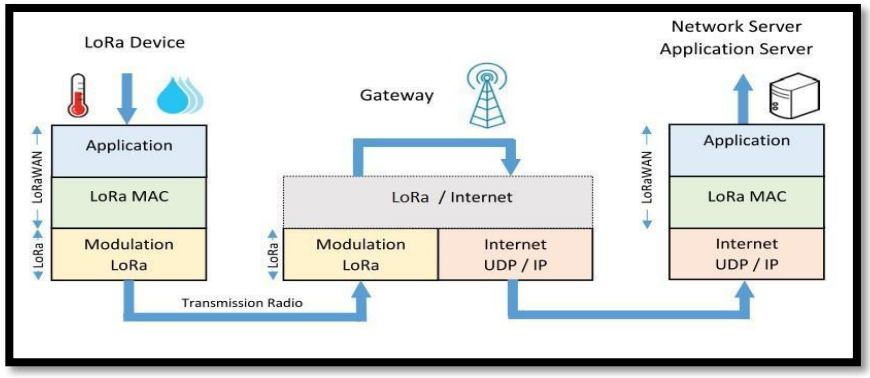

Figure 12: The Role of LoRaWAN Gateway.

3. The Network Server (NS):

After receiving the message from the Gateways, the Network Server discards any duplicates (originating from various Gateways). [18] Network Session Key: NwkSKey, a 128-bit AES key, is used to authenticate LoRaWAN packets.

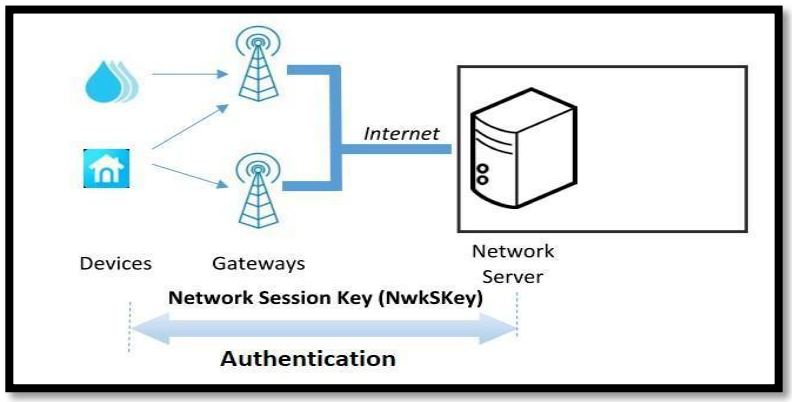

Figure 13: Network Session Key Authentication.

4.The Application Server:

It keeps the applications apart from one another. The application server can be used to store data (Frame Payload) from the registered LoRa devices. Application Session Key: AppSKey, a 128-bit AES key, is used to encrypt the communications in this instance.

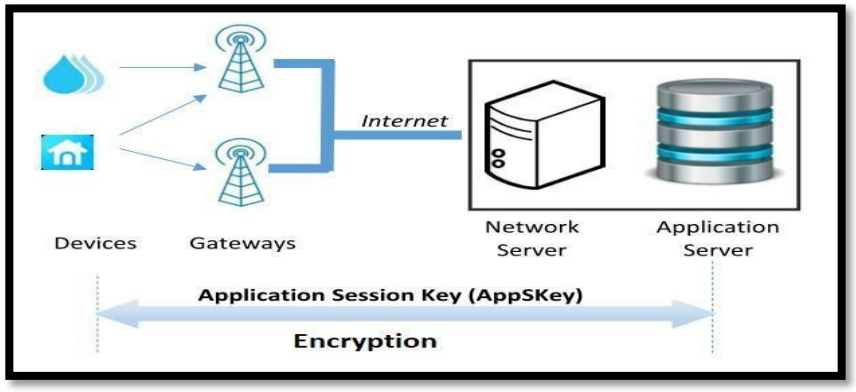

Figure 14: Application Session Key Encryption.

2.4 LoRaWAN PACKET FORMAT:

We simply do not send the data directly using the LoRa Modulation, instead, there must be a frame for our data. The Frame of the LoRa Packet consists of:

- A preamble to allow the receiver to synchronize.
- Optional header (Used in the explicit mode)
- Data Payload
- CRC fields (checking the integrity of the frame).

The LoRa protocol data is called PHY Payload (physical layer data). A general overview of the LoRa frame would look as in figure 14.

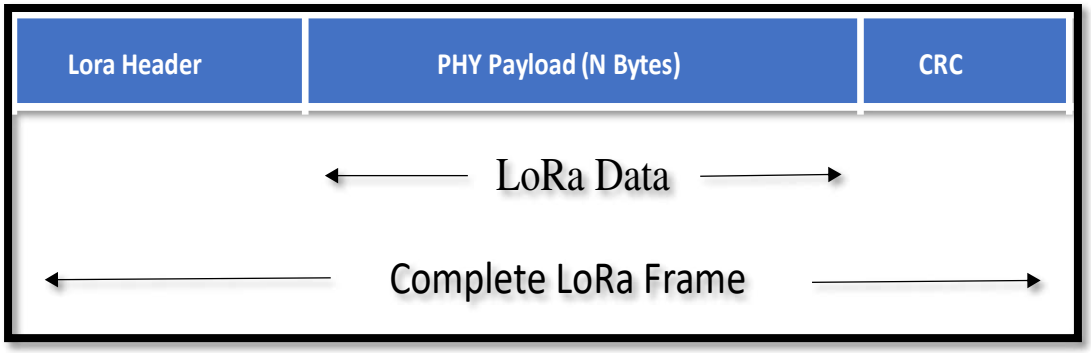

Figure 15: Lora Packet format.

As LoRaWAN is a different layer protocol than LoRa then the frame has to be modified. A simple general view for the LoRaWAN frame would look like in figure 15.

Figure 16: LoRaWAN Simple Packet format.

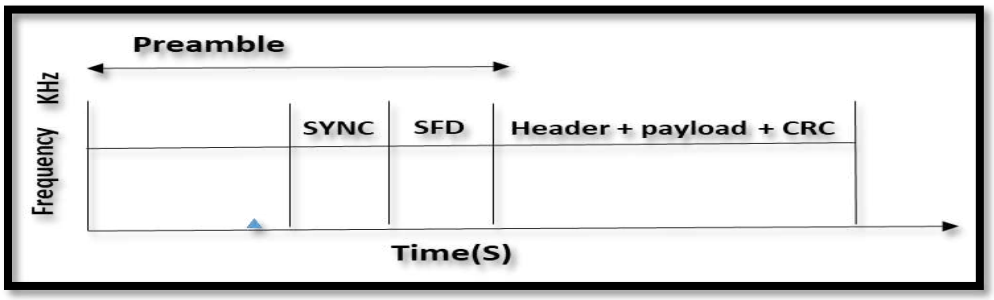

Figure 17: Spectrum Analyzer view of the Frame [19].

The Preamble is mandatory for every transmission to synchronize the receiver with the incoming data flow. By default, the packet is configured with 12.25 symbols long sequence [20]:

- 8 configurable symbols (preamble)
- sync word symbols
- 2.25 SFD symbols.

CHAPTER-3

3.1 LoRa MODULATION AND DEMODULATION:

In theory, modulation refers to the process of altering the characteristics of a carrier signal in alignment with the instantaneous values of the modulating signal, which could be either a digital or analog information-carrying signal. For analog signals, various modulation methods are employed, including Amplitude Modulation (AM), Frequency Modulation (FM), Phase Modulation (PM), and combinations. Likewise, digital signal modulation techniques can be applied, such as Amplitude Shift Keying (ASK), Frequency Shift Keying (FSK) [21], and Phase Shift Keying (PSK).

In the context of LoRa technology, FSK is employed, where a binary "1" is conveyed through one frequency, and a binary "0" is conveyed through another frequency, as depicted in Figure 18.

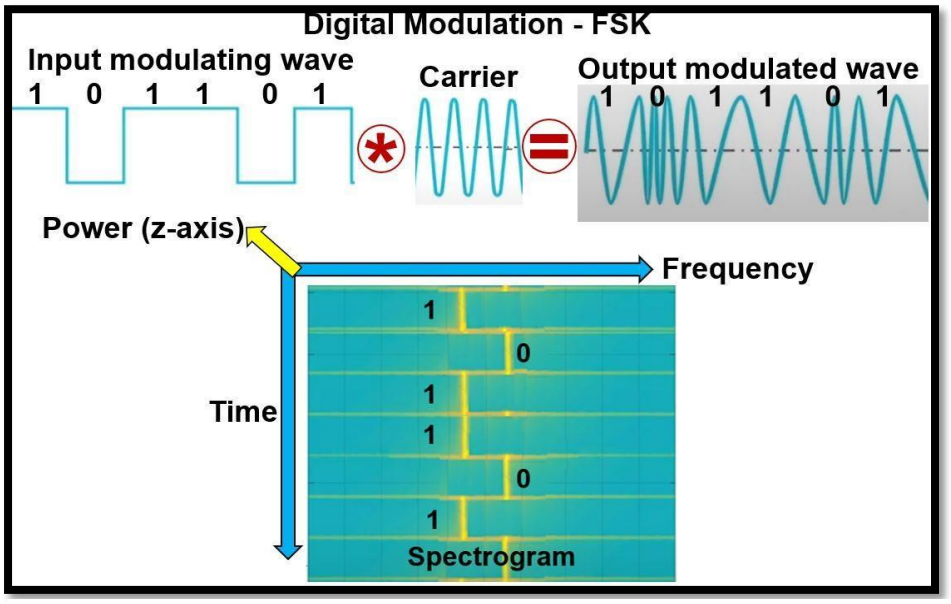

Figure 18: FSK Modulation.

The LoRa physical layer employs the [22] Spread Spectrum Modulation technique, specifically based on Chirp Spread Spectrum modulation, a proprietary method developed by Semtech. This approach allows for the transmission of data at various rates without causing interference. It achieves this by utilizing wideband linear frequency-modulated Chirp pulses to encode data. In simpler terms, the CSS technique involves spreading the signal across the frequency domain.

A Chirp, also known as a sweep signal or sweep rate, governs how the signal's frequency changes over time. There are two types of chirps: the up chirp (for increasing frequency) and the down chirp (for decreasing frequency), as depicted in Figure 19. Notably, the chirp technique finds applications in marine and military radars and the open-source GNU Chirp Sounder.

In the United States, [3] LoRa specifies bandwidth values of 125 kHz, 250 kHz, and 500 kHz. Conversely, in Europe, the options are more limited, with 125 kHz and 250 kHz being available. Figure 17 illustrates the sweep signal duration for various combinations of bandwidths (125 kHz, 250 kHz, 500 kHz) and spreading factors (ranging from 7 to 12).

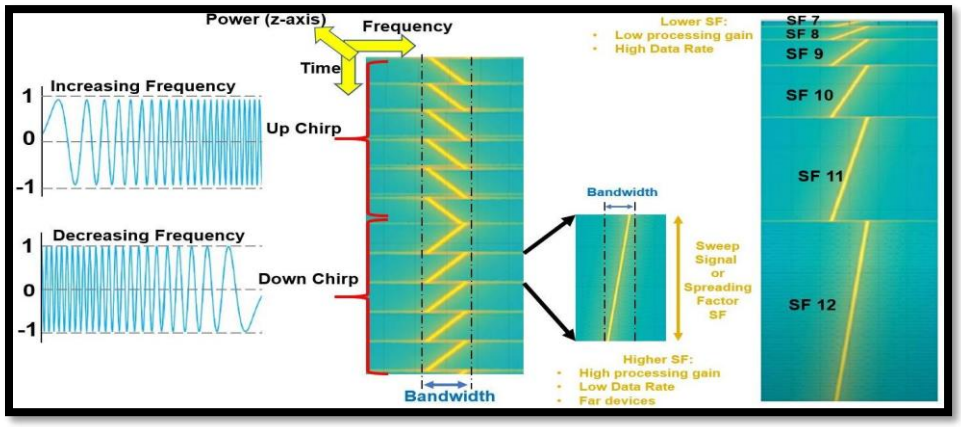

Figure 19: Up Chirp and Down Chirp [22]

CSS modulation provides the following advantage [23]:

- Greater link budget
- Resilience to interference
- Performance at low power communication link
- Doppler effect (for motion sensor applications)
- High receiver sensitivity

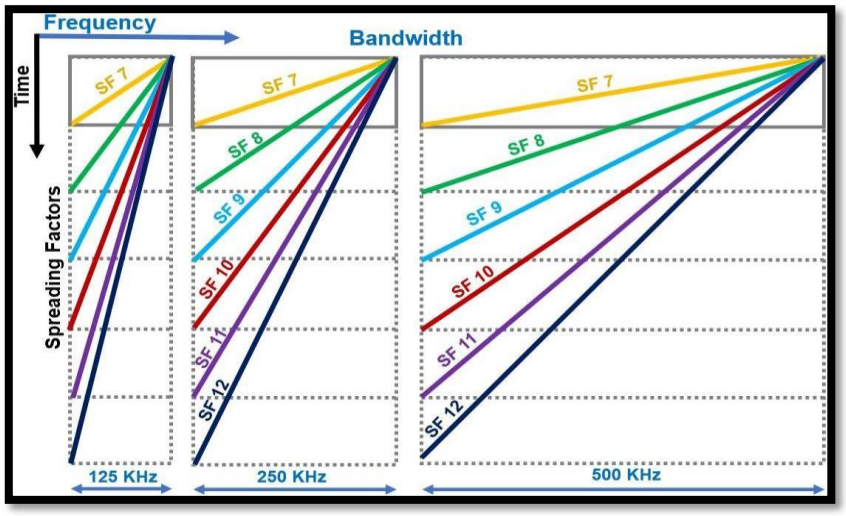

Figure 20: Illustration of the Sweep Signal Length.

Table 1: Keyword and Definitions

Keyword	Definition
Symbol	Discrete RF energy state to represent quantity of data (one or more bits)
Possible Symbols Example	2^{SF} values. One value is encoded into an Up Chirp (sweep signal) 2^7= 128 values (1 bit has two states "0" or "1", SF = 7)
Data Encoding	Symbols represent encoded data. Data is transformed before TX.
Bandwidth	Width of radio spectrum occupied by chirp into the frequency domain
Spreading Factor	Quantity of bits encoded per symbol; US: 7 to 12

The physical structure of a LoRa frame comprises three key components: the preamble, synchronization bits, and the payload. The preamble commences with eight up chirps, serving as the transmission's starting point. Following the preamble, two down chirps, known as synchronizing symbols [23], follow. This combination of chirps is universally recognized by any LoRa gateway as the initiation of a packet transmission, effectively grabbing its attention. Subsequently, the actual data transmission commences, employing chirps that traverse the bandwidth in an arbitrary manner. In essence, the data harnesses chirp spread spectrum technology for its transmission, as visually represented in Figure 21.

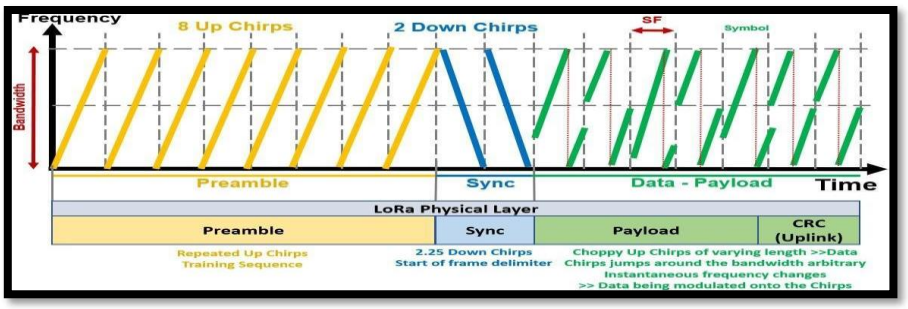

Figure 21: LoRa Physical Frame

The use of the lowest Spreading Factor (SF=7) results in the highest data rate because it involves sending more chirps per second, thereby allowing the system to encode a greater amount of data in the same time frame. The advantage of this higher data rate is that the signal's lower energy levels enable it to travel further over shorter distances.

Conversely, opting for a higher Spreading Factor (SF=12) signifies fewer chirps being transmitted per second, equating to a lower data rate. However, this extended transmission duration allows the signal to cover greater distances, as illustrated in Figure 22. This prolonged airtime results in enhanced sensitivity, ultimately leading to expanded coverage, making it possible for the sensor to detect the signal from a greater distance. Notably, the link budget experiences a 2.5 dB increase with each increment in SF.

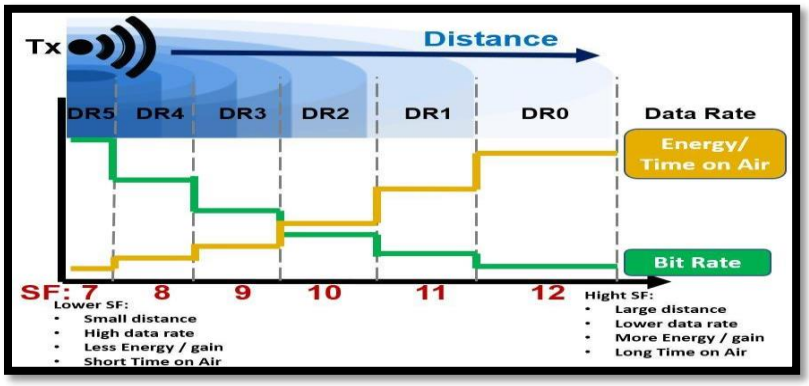

Figure 22: Energy vs. Bit Rate [24]

The LoRa demodulator, in its process of signal reception, undertakes the task of de-chirping the incoming signal to recover the original transmitted signal. This entails determining the positions of the chirp transitions. The initial step involves extracting the data from the LoRa packet and subsequently de-chirping it, thereby distinguishing and isolating the preamble, synchronization elements, and the payload data.

Operating at the appropriate Spreading Factor (SF) and Bandwidth (BW), the demodulator generates both Up and Down chirps. For instance, the original signal (fo) is multiplied by its complex conjugate (-fo), resulting in a signal of "0" (fo * -fo = 0), signifying a constant value. Consequently, the LoRa signal is individually multiplied by Up and Down chirps (in accordance with the selected SF). In simpler terms, this entails multiplying the received LoRa signal by the Inverse chirp, leading to the de-chirped signal. Subsequently, the de-chirped signal undergoes a Fast Fourier Transform (FFT), with the FFT duration matching the number of potential symbols [23]. This process effectively identifies the desired symbol as the component with the highest energy or power within each FFT. The modulation procedure is visually depicted in Figure 23 [23].

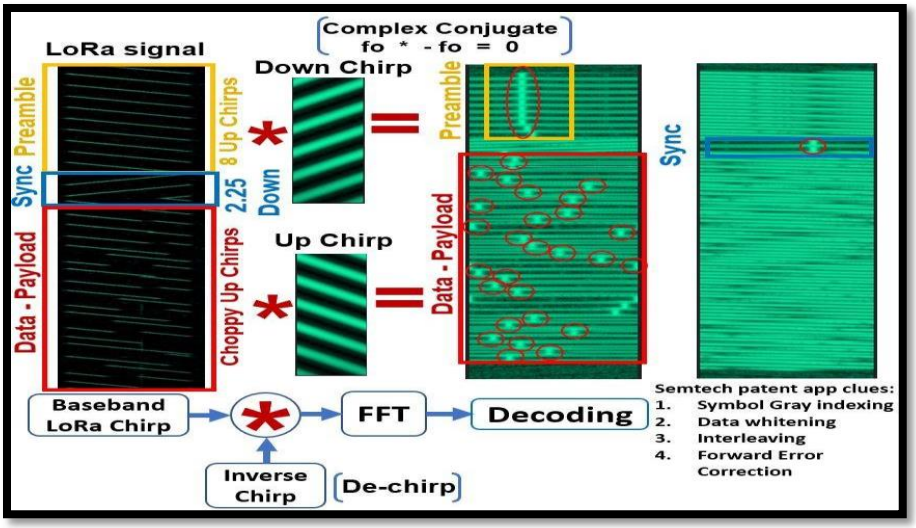

Figure 23: LoRa Demodulating [23]

3.2 LoRaWAN Regional Parameters:

International entities are responsible for the management of the radio spectrum to ensure the compatibility and interoperability of radio technologies. Additionally, individual countries' local telecommunications regulatory agencies may impose specific additional constraints and parameters.

In Europe, for instance, this role is fulfilled by the European Telecommunications Standards Institute (ETSI), which sets the maximum allowed transmission power for uplink signals at 25 mW (14 dBm) and 0.5 W (27 dBm) [25]. In the United States, the Federal Communications Commission (FCC) oversees the regulation of interstate and international radio transmissions, including television, wired, satellite, and cable communications across all 50 states, the District of Columbia, and U.S. territories. The primary responsibility of the FCC is to process applications and grant licenses for operating on specific frequencies and using specific technologies [26].

In the Federal Communications Commission (FCC) enforces the FCC Part 15 standards for the 902 - 928 MHz Industrial, Scientific, and Medical (ISM) band, often referred to as the 915 MHz ISM Band. The frequency plan is outlined in Table 2 and visually represented in Figure 26 [27]. For the purposes of this thesis, channel eight (8) is designated as the up-link channel, operating at a frequency of 903.9 MHz.

Table 2: US 902-928 MHz Frequencies Plan

Description	Upstream – 64	Upstream – 8	Downstream – 8
Channels numbered	0 to 63	64 to 71	0 to 7
Number of channels	64	8	8
Frequency starting at	902.3 MHz	903.0 MHz	923.3 MHz
Linearly increment	200 kHz	1.6 MHz	600 kHz
Frequency ending at	914.9 MHz	914.2 MHz	927.5 MHz
Bandwidth	125 kHz	500 kHz	500 kHz
SF varying	SF7 - SF10	SF8	SF7 - SF12
Coding rate	4/5	4/5 - 4/8	4/5 - 4/8

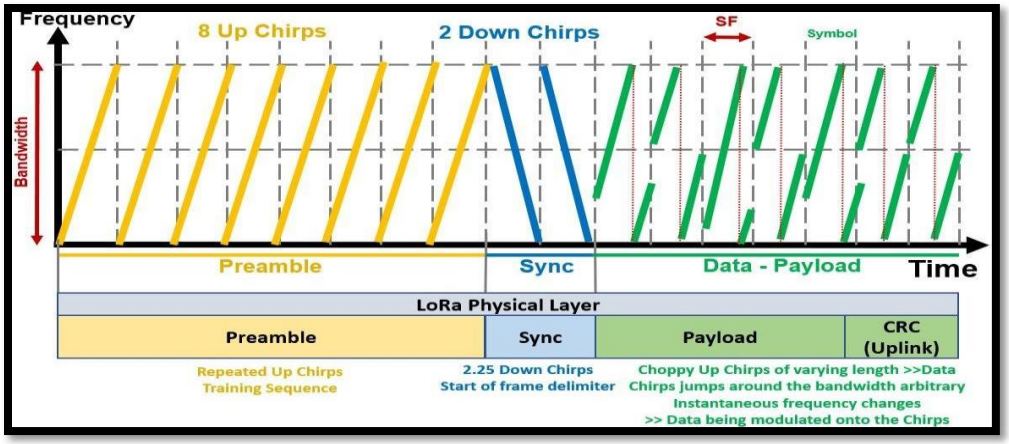

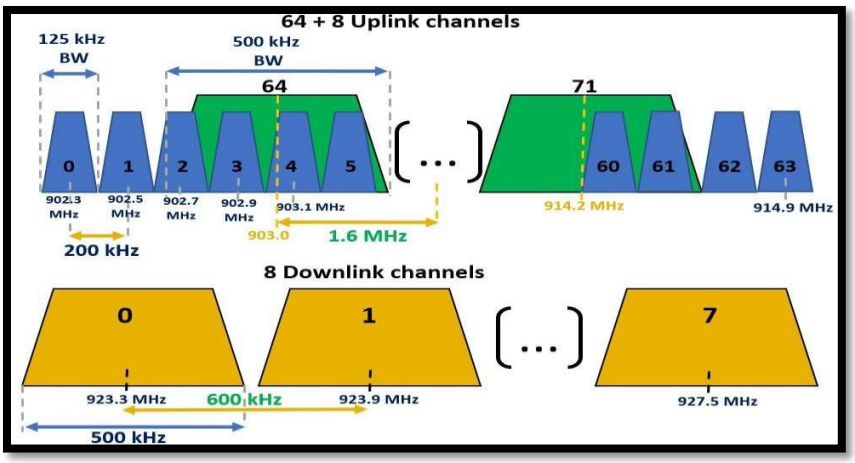

Figure 24: US 902-928 MHz Frequencies Up-link and Down-link.

The end-devices are demanded to operate under regulatory specifications for the 915 MHz ISM band by FCC. Table 3 shows a succinct description of the principal regulations on the 915 MHz ISM bands, as well as Table 4 presents characteristics for LoRaWAN on US 902-928 MHz frequencies [28].

Table 3: LoRaWAN Regulation for North America

Description	LoRaWAN specification for North America and EU
Frequency Band	868 /902 - 928 MHz
Max. TX Power Up-link	(30 dBm allowed) 20 dBm is typical
Max. TX Power Downlink	27 dBm
Max. dwell time	400 milliseconds on Up-Links

Table 4: US 902-928 Channel LoRa Characteristics

Data Rate (DR)	Spreading Factor (SF)	Bandwidth (KHz)	Up-link or Down-link	PHY Bit Rate (bits/sec)	Maximum MAC Payload (Bytes)
0	SF 10	125	Up-link	979	11
1	SF 9	125	Up-link	1,759	53
2	SF 8	125	Up-link	3,124	125
3	SF 7	125	Up-link	5,471	242
4	SF 8	500	Up-link	12,501	242
5 - 7	Not defined				
8	SF 12	500	Down-link	980	53
9	SF 11	500	Down-link	1,760	129
10	SF 10	500	Down-link	3,125	242
11	SF 9	500	Down-link	5,470	242
12	SF 8	500	Down-link	12,500	242
13	SF 7	500	Down-link	21,900	242

CHAPTER-4

4.1 Deployments, Coverage and Advantages of Lora Technology:

4.1.1 Lora Deployments:

Low-power wireless technology, with a particular focus on the LoRa/LoRaWAN standard's experimental architecture and the availability of hardware for rapid development and experimentation. In recent years, collaboration between the business sector and academia has significantly elevated the prominence of LoRa transmission.

The following table provides insights into the implementation of LoRa applications across various domains, including smart agriculture, smart metering, environmental monitoring, and appliance control. In reference [38], researchers have developed a comprehensive LoRa-based system for monitoring large-scale agricultural farms, rigorously examining the reliability of the associated hardware, software, and platform for remote farm monitoring [39]. In another study, authors established a smart metering infrastructure based on LoRa, meticulously assessing both cost and energy consumption implications.

Furthermore, the deployment of a LoRa-based atmospheric monitoring system is highlighted in reference [40], with researchers evaluating system performance metrics, such as end-to-end throughput delay. Similarly, in reference [41], a LoRa-based smart appliance monitoring and control system was designed and subjected to scrutiny, particularly in terms of power consumption.

In the realm of plant research, LoRa's potential has been demonstrated convincingly in reference [42]. Additionally, references [43], [44], and [47] outline an IoT-monitored architecture reliant on the LoRa standard for the remote administration of offshore sea fields. Moreover, the potential for achieving smart irrigation using LoRa is explored, with analogous approaches detailed in references [45] and [46] for monitoring systems in field applications.

Table 5: Lora Deployments

Reference	Year	LoRa Deployments	Assessments
[38]	2022	Monitoring of large-scale agriculture farms	Examine remote. monitoring with Risibility
[39]	2021	Smart metering	Cost and energy analysis
[40]	2021	Ecological monitoring in infrastructure-less areas	Analysis of performance metrics
[41]	2021	Monitoring of appliances	Examine power usage
[42]	2020	Crop monitoring	Analyze power. consumption
[43]	2020	Monitoring of sea farm	Assessment of scenarios
[44]	2020	Water management	Examination of experimental performance
[45]	2020	Monitoring of crops and plants	Analyze the environmental impact
[46]	2020	Monitoring the crop	Assessment of energy usage
[47]	2019	Irrigation management	Valuation of experimental results

4.1.2 Coverage of LoRa:

LoRa technology's flexibility, long-range capabilities, and efficient power consumption make it a versatile choice for a wide range of IoT deployments, and careful planning and optimization can ensure optimal coverage for specific use cases.

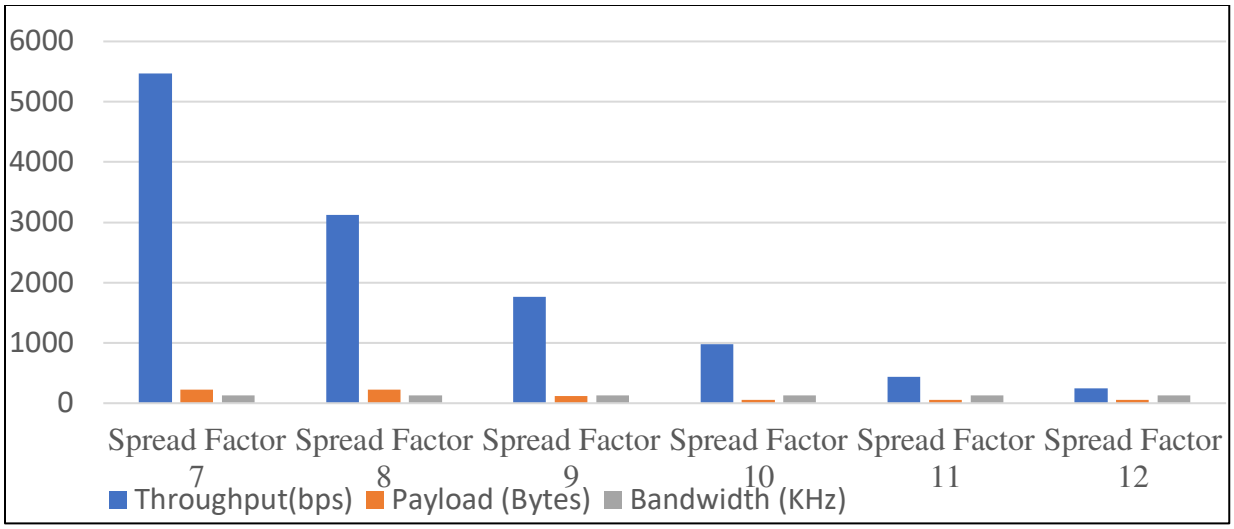

Figure 25:Relationship among throughput, payload, and bandwidth with spread factor.

The evaluation of [3] LoRa's range encompasses various metrics, including transmitted signal intensity, signal-to-noise ratio (SNR), and packet transit rate. SNR serves as a crucial indicator of connection quality in a wireless network's atmospheric conditions [48]. In the context of smart cities, the service zones required for IoT devices vary based on technology type, device location, and communication style (e.g., point-to-point or gateway interfaces). These factors are linked to the platform's design specifications. As part of our performance assessment, healthcare solutions, for instance, prioritize stable interactions between a screening framework and a central node.

However, certain applications, such as those focusing on real-time patient follow-up, demand signal efficiency for seamless communication, especially when devices are in motion [49]. The coordination of intelligent street lighting equipment for mobility or traffic management applications necessitates connectivity between multiple terminals within a confined area. The optimal spacing between traffic lights is approximately 35 meters [50]. In the realm of smart parking, a user's location can be determined using the Received Signal Strength Indicator (RSSI) level, even without the use of a dedicated smart device [51]. A high RSSI value indicates proximity to a vacant parking space.

The accompanying figure illustrates the relationship between throughput, payload size, and bandwidth in the context of LoRa technology. As the spread factor increases, both throughput and payload size decrease. For instance, when the payload size is 230 bytes with a bandwidth of 125 kHz at the 868 MHz band and a Spread Factor of 7, the throughput reaches 5470 bps. However, when the spread factor is increased to 12, the payload shrinks to 59 bytes, resulting in a lower throughput of 250 bps.

4.1.3 Communication Scalability and Reliability:

In the context of uplink communication within dense LoRaWAN deployments, it becomes evident that communication scalability presents a significant challenge. As the number of end nodes within the network increases or the traffic load grows, a corresponding rise in the number of packet losses occurs. Moreover, the average power consumption per end node increases, thus diminishing the battery lifetime to levels below acceptable thresholds. This issue primarily arises from the Aloha-based access scheme employed by LoRaWAN.

To enhance scalability beyond the tuning of the ADR (Adaptive Data Rate) mechanism in the current LoRaWAN, alternative transmission synchronization solutions come into play. These solutions encompass approaches like slotted Aloha access schemes for uplink [52], beacon-based time-synchronized uplink communication [53], various polling-based techniques [54], and even more finely grained scheduling possibilities [55]. The latter method not only bolsters scalability but also elevates reliability by preventing interference with scheduled traffic due to other LoRaWAN transmissions. An advanced step, building upon [55], could involve coordinating transmissions across different network technologies to mitigate inter-technology interference within LoRaWAN.

The usage of confirmed traffic within LoRaWAN leads to increased spectrum occupancy since many packets necessitate retransmission due to the absence of downlink confirmation. While the LoRaWAN standard [56,57] mandates that confirmation is to be transmitted in receive windows following the uplink transmission, a lack of confirmation does not necessarily indicate uplink packet loss. Instead, it is often linked to gateway duty cycle. To address this, a desirable approach is to have the confirmation traffic follow a mechanism similar to ADR, wherein the end node awaits confirmation in subsequent D uplink packets.

This approach provides gateways with the flexibility to confirm uplink traffic later, alleviating the immediate confirmation requirement. Furthermore, group confirmations for previous uplink packets can be implemented.

In Europe, radio duty cycle regulations pose an additional obstacle to LoRaWAN scalability, particularly in the context of downlink communication. Implementing carrier sensing mechanisms in gateways can eliminate the need for radio duty cycles in the downlink [58,59]. While this simplifies duty cycle requirements, hidden-node issues remain unresolved due to the vast coverage. Nonetheless, such mechanisms fall short of ensuring high reliability in downlink communication. To improve downlink scalability and reliability, collision avoidance-based techniques [60,54] can be employed, albeit at the cost of increased average power consumption for end nodes. packet collisions between uplink and downlink traffic are possible through the isolation of UL/DL communication in distinct sub-bands [61]. Furthermore, allocating high-power, high-duty cycle channels for the first receive window in downlink can improve scalability while reducing power usage.

To mitigate the negative impact of duty cycle on downlink traffic, a solution involves co-locating multiple gateways to increase downlink duty cycles. These co-located gateways require centralized management to control channel usage and SF (Spreading Factor) assignments in the downlink, preventing collisions. Advancements in electronics open the possibility of simultaneous transmissions using different SFs and channels by a single gateway, employing a time-power multiplexing approach [61] to reduce gateway duty cycle.

In highly dense networks, the ADR scheme may lead to a situation where most end nodes switch to the highest SF, significantly increasing the likelihood of collisions. In such cases, adopting a static SF assignment approach becomes beneficial. By maintaining a portion of end nodes with static SFs and allowing others to use ADR, the detrimental impact of ADR in congested networks can be mitigated.

4.2 ADVANTAGES:

The proposed network specification for expanding networks with intermediate nodes offers several distinct advantages when compared to the alternative of adding extra gateways. These advantages are as follows [63]:

1. Cost-effectiveness and Ease of Installation:

Intermediate nodes can be manufactured in expensively, and their integration into the LoRaWAN network is straight forward, akin to any other LoRaWAN device. In contrast, an additional gateway incurs significantly higher costs, both in terms of hardware and ongoing operational expenses. [62] Monthly subscription fees for a gateway, covering backend and backbone services, can easily exceed the expenses associated with an intermediate node.

2. Uniform Hardware:

The specification is designed to be lightweight and easily implementable on the same hardware used for end-devices. Consequently, the primary distinction between an intermediate node and an end-device lies in whether the device is equipped with software to function as an intermediate node or not. This flexibility facilitates the repurposing of end-devices into intermediate nodes, or vice versa, if the need arises. The primary hardware addition recommended for intermediate nodes is a larger battery to accommodate the heightened energy consumption resulting from their continuous listening capability and increased transmission rate, in comparison to end-devices.

3. No Additional Backbone Connection Required:

Unlike a gateway, an intermediate node does not necessitate any supplementary backbone connections, as it functions as a relay node towards the gateway, which maintains a stable backbone connection. The gateway's backbone connection can either be directly linked to the internet via an Ethernet cable with network access or through a 3G network. These backbone connections may be challenging to find or costly to establish at the desired location for a gateway, making the intermediate node a more viable choice.

4. Enhanced Battery Efficiency:

Intermediate nodes, featuring simpler hardware and the sole task of monitoring a single frequency and spread factor (SF), consume significantly less power compared to a gateway. This attribute holds paramount importance, especially since intermediate nodes are often deployed in remote, power-constrained locations.

5.Environmentally Responsible:

Intermediate nodes, due to their streamlined hardware design, contribute to a reduction in resource consumption and generate less waste compared to gateways. Furthermore, as previously mentioned, they exhibit lower power consumption during operation, which aligns with environmentally conscious practices.

4.3 LORAWAN VERSIONS:

There are different versions of LoRaWAN Specifications.

- LoRaWAN Specification v 1.0 (Already withdrawn).
- LoRaWAN Specification v 1.0.1 (Certification towards 1.0.1 has ended).
- LoRaWAN Specification v 1.0.2 (First stable version Suits Most Class A or C users).
- LoRaWAN Specification v 1.0.3 (Fully supports unicast and multicast Class B devices. Class A and Class C unchanged compared to 1.0.2 with the exception of a new MAC command, if you use Class B you may need this).
- LoRaWAN Specification v 1.1.

CHAPTER-5

5 RESEARCH AIM:

In order to effectively manage, monitor, and protect the marine ecosystem, it is essential to utilize real-time measurements that encompass multiple variables, as well as advanced physical and ecological numerical modeling tools.

Permanent ocean observatories play a crucial role in operational monitoring, particularly when high-frequency measurements, multiple parameters, and data spanning from the sea surface to the ocean interior and sea-floor are necessary.

Figure 26:Mediterranean Moored Multi-Sensor Array, also known as W1M3A

The W1M3A observing system is a vital infrastructure for the National Research Council of Italy and is affiliated with ERIC EMSO and ERIC ICOS. Located in the center of the North Western Mediterranean Sea, approximately 80 Km offshore on a seabed 1200 m deep, the observatory monitors meteorological conditions and the physical and biogeochemical status of the ocean in the region.

5.1 POSITION:

The mooring position at W1M3A is located at the intersection of various commercial routes. The observatory is situated in a highly exposed area, facing winds and waves from both the Gulf of Lion and the Italian seas without any natural barriers for protection.

Due to its strategic location, the observatory is ideally positioned for collecting data on sea waves and offshore winds. It also serves as a valuable tool for detecting early warning signs of inclement weather and gathering long-term meteo-oceanographic data.

5.2 INTRODUCATION:

Monitoring the marine environment is crucial in gaining a better understanding of the intricate ecosystems that have a direct influence on climate and human activities. With the advancement of innovative, small, and energy-efficient sensors, along with the urgency to comprehend the effects of [6] climate change in recent years, the monitoring of oceans has evolved. Significant strides have been taken to establish stationary or mobile platforms capable of conducting simultaneous measurements of various parameters like atmospheric over extended periods with high accuracy and frequency.

Oceans are still under sampled, despite the fact that there are currently more than 1300 monitoring devices and 1400 floats operating at sea worldwide [64]. The risks and losses associated with inadequate and non-sustainable ocean observation and data collecting have been highlighted by a number of recent European intergovernmental initiatives [65].

Nowadays, the common priority for all existing networks of observing systems, monitoring strategies, and development of innovative sensors is therefore to create mechanisms and technologies such that data has greater societal and scientific value, and the overall life cycle cost of sensors and observing systems is reduced [66–67].

The high cost of data transmission from sea platforms to shore using either short-range local base stations or standard satellite communication, which consumes a lot of power, is one of the most difficult difficulties in this type of environment. Battery-powered devices are unable to utilize the former strategy, and the latter is more expensive because it needs to physically connect to the local base station in order to transmit data [68].
Building and supporting networks of far-away marine sensors has made extensive use of both radio systems and cellular terrestrial networks; for instance, [22] Worldwide Interoperability for Microwave Access (WiMAX) is employed in places that are not covered by satellites [69,70]. In order to develop Wireless Coastal Area Networks (WiCAN), a mix of WiMAX, Long-Term Evolution (LTE), and Very High Frequency (VHF) has been suggested.

A highly attractive technology that utilizes radio coverage over open spaces and necessitates extremely low energy consumption is the Low-Power Wide Area (LPWA) network. This is becoming more and more popular as a useful method of enabling machine-to-machine interaction in rural as well as urban environments [71,72].

LPWA networks are built on the interaction and data sharing of heterogeneous devices through a layered architecture, enabling long-range communications for the Internet of Things (IoT) [73]. The design of a two-way communication channel supporting the use of adaptive network topologies that can alter their operation in terms of sampling strategy or extension of the area to be controlled, depending on changes in the environment, is necessary to develop an ICT platform compliant with the IoT concept to be applied in the marine environment. In fact, IoT systems for marine applications must be designed to take use of heterogeneous sensors that are intelligent, networked via LPWA, and capable of disseminating data extensively [74, 75].

Expanding LPWA networks ability to offer new technological solutions hardware, software, and middleware components to be applied to platforms and sensors for broad-spectrum marine monitoring is one of the main drivers of their use for maritime applications. This may encourage the quick use of information and offer innovative basin-scale services like water quality assessment or vessel control in designated regions with specific navigational

restrictions (marine protected areas and off-limits zones, for example). In order to do this, specific tests have been conducted that take advantage of Long Range (LoRa) technology's inherent ability to offer dependable connection across the ocean for a few miles [74–76].

The network performance has been assessed both during a research trip that took place in the Northwestern Mediterranean Sea in last October and while it was tracking the route of a passenger ship that had IoT end nodes installed.
It was possible to track the route of a boat fitted with GPS-IoT end nodes near the coast using several gateways running concurrently on land using the developed LoRa network. It was also possible to show that it is feasible to transmit meteorological and oceanographic data using IoT end nodes deployed at sea and installed on an existing observatory up to 100 km away from the coast.

5.3 MATERIAL AND METHODS

5.3.1. LoRa and LoraWAN:

Among operational LPWA network technologies, [85] the LoRa solution gives the best technology for the implementation of private IoT networks that can be implemented ad hoc without the need for proprietary licenses, with the ability to utilize three classes of devices in order to guarantee efficient energy management depending on the area of application and to allow resilience to interference [29].

LoRa technology gives a robust modulation that allows the use of receivers with very low sensitivity (Rx_{sens}) of the order of 140 dBm through the utilization of frequencies in the sub-GHz band (nominally 868 MHz for Europe).

The value given indicates the recognized minimum power required for reliable transmission and may be computed using the equation:

$$Rx_{sens} = -174\ dBm + 10.\log(BW) + NF + SNR$$

(5.1)

where BW represents the bandwidth in kHz, NF is the noise factor in decibels dB, and SNR is the signal to noise ratio in decibels dB.

Under the free space hypothesis, the simplest model for estimating the power of the LoRa packet received at the gateway is based upon the Friis transmission equation:

$$P_{rx} = Tx_{power} - Path_{loss} + G_{Tx} + G_{Rx}$$

(5.2)

where Tx_{power} represents the transmitted power (dB), $Path_{loss}$ is the free space power loss because of the channel (dB), and G_{Tx} and G_{Rx} represent the antenna gain in transmission and reception (dBi). The received power at the gateway is sometimes represented as the Received Strength Signal Indicator (RSSI).

The log-distance path model, which may be estimated using the following equation, is the simplest model for estimating the $Path_{loss}$term in free space:

$$Path_{loss} = 20.log_{10}(d) + 20.log_{10}(f) - 147.55$$

(5.3)

where d is the distance between the transmitter and the receiver (in meters), and f is the effective transmission frequency (in hertz).

The Hata model [30] is a more accurate representation that can be used in wireless communication systems for microwave radio links having frequencies up to 1500 MHz and ranges up to 100 km. $Path_{loss}$ can be calculated in situations with no barriers using the following approximation:

$$Path_{loss} = 69.55 + 26.16.log_{10}(f.10^{-6}) - 13.82.log_{10}(h_B) - C_H$$
$$+ (44.9 - 6.55.log_{10}h_B).log_{10}(d.10^{-3})$$
$$-4.78.(log_{10}(f.10^{-6})^2 + 18.33.log_{10}(f.10^{-3}) - 40.94$$

(5.4)

where hB is the base station antenna is altitude in meters and C_H is the antenna height correction factor. The following equation can be used to approximate the value of C_H in a semi-urban area, such as the one in which the experiment was carried out:

$$C_H = 0.8 + (1.1 \cdot \log_{10}(f \cdot 10^{-6}) - 0.7) \cdot h_M - 1.56 \cdot \log_{10}(f \cdot 10^{-6})$$

(5.5)

where hM is the node antenna's altitude (in meters).

The expression of $Path_{loss}$ for the Hata model modifies with the presence of a radio path over a semi-urban area, as shown by the following equation:

$$Path_{loss} = 69.55 + 26.16.log_{10}(f.10^{-6}) - 13.82.log_{10}(h_B) - C_H$$
$$-13.82.log_{10}(h_B) - C_H + (44.9 - 6.55.log_{10}h_B).log_{10}(d.10^{-3})$$
$$-2.\left(log_{10}\left(\frac{f.10^{-6}}{28}\right)\right)^2 - 5.4$$

(5.6)

The European Conference of Postal and Telecommunications establishes a maximum transmission power of 25 mW (14 dBm) for uplink messages and 0.5 W (27 dBm) for downlink messages, as well as a maximum allowed antenna gain of 2.15 dBi, in the recommendation ERC-REC-70-3E.

Furthermore, depending on the channel used, the proportion of time an IoT device can be operated, commonly referred to as duty cycle, must be limited to 0.1% to 1% per day [31].

A LoRa transmission is physical layer is based on the Chirp Spread Spectrum (CSS) modulation, which is also utilized for radar applications. The signal's characteristic is an up- or down-chirped signal that changes in frequency over the course of the band's transmission. The encoding network (CR, variable from 1 to 4 depending on the code rate chosen among 4/5, 4/6, 4/7, and 4/8), which indicates the redundancy applied to the data, the band used (BW, kHz), and the Spreading Factor (SF, variable from 6 to 12) that represents the number of bits encoded per chirp are the parameters that characterize CSS modulation. These elements influence the LoRa transmission's bit rate (BR) in the following equation:

$$BR = SF.\frac{\frac{4}{4+CR}}{\frac{2^{SF}}{BW}}.1000 \tag{5.7}$$

Depending on the application, the ideal combination of the various parameters must be chosen, with an increase in data rate resulting in a decrease in SF and an increase in dependability resulting in an increase in SF and, as a result, a higher SNR.

LoRa communication is encoded with the following parts: (1) a preamble of (8) up-chirps encompassing the entire band, the last two of which compose the synchronization word (sync word) required to distinguish the various network nodes accessing the channel as a shared resource; (2) Time synchronization symbols consisting of two down chirps and a quarter of down chirps for a length of roughly 2.25 symbols. (3) header (H), which is an optional field containing the size of the payload, the coding rate used, and whether or not the 16-bit Cyclic Redundancy Check (CRC) control code is enabled; (4) payload (PL), which can be up to 255 bytes. To determine the number of symbol (Rn_s) in the payload, use the following equation:

$$Rn_s = 8 + \max(\frac{(8.PL - 4.SF + 8\,CRC + H)}{4.(SF - DE)}.(CR + 4), 0)$$

(5.8)

where H is 20 if present or 0 otherwise, DE is 2 if the data rate optimization technique is activated with SF larger than 11 or 0 otherwise.

The LoRaWAN media access control (MAC) layer communication protocol provides an upper-level layer to LoRa technology that is necessary for geolocation applications based on measurements of the time difference between the arrival of the same signal at multiple gateways (TDOA) or the power of the same signal received (RSSI) from multiple gateways. Particularly, LoRaWAN is an open standard that specifies the LPWA network's communication protocol based on a LoRa chip, which regulates the link layer MAC using a pure ALOHA type algorithm.

The use of the LoRaWAN protocol implies that there is no return channel, that the channel access time is divided into intervals, that the first packet at the head of the queue is transmitted, and that if a confirmation message (ACK) is needed, the end-node can retransmit the data after a random time interval.

The star or star-of-star topology is the most often used LoRaWAN topology, in which communications from a single end-node are routed to a central server via a gateway without numerous hops. Because end-nodes transmit regardless of the number of gateways that may receive the packet, point-to-point communication between the end-node and the gateway is not permitted.

Each gateway that detects a LoRaWAN message passes the data to the network server with which it is attached. The server is in charge of redundancy detection, security checks, and message scheduling. The network nodes can communicate over the channel at the same time as long as they use distinct frequencies or SFs. Because the end-node sends data directly to numerous gateways, this topology makes resource tracking easier. The LoRaWAN network setup involves a secure and organized system for communication between end-nodes and the central server. Each node has unique identifiers, such as the 64-bit DevEUI and AppEUI, which help in distinguishing them within the network. When a node joins the network, it's

assigned a unique 32-bit address by the server and receives security keys like the (NwkSKey) and (AppSKey), both utilizing AES encryption to ensure the integrity and confidentiality of messages.

The NwkSKey, shared between the node and the server, secures the integrity of messages on the network, while the AppSKey, also AES encrypted, is necessary for encrypting and decrypting the information transmitted by the node, ensuring the confidentiality of the data being communicated.

This approach seems robust in terms of security and encryption, as it employs AES encryption for both network integrity and data confidentiality, along with unique identifiers for each node and centralized management through the server.

When an end-node requests to join the network, it typically starts at a lower data transmission speed (SF equals 12), resulting in a slower transmission but providing a higher interval for sending the same amount of information. Once [82] the LoRaWAN server confirms the end-node's network membership through an acknowledgment, the data transmission adjusts to reduced Spreading Factors (SFs) based on channel noise and estimated distance between the gateway and node, optimizing transmission efficiency.

There are two methods for an end-node to register on the network: [81] "Over the Air Activation" (OTAA) and "Activation by Personalization" (ABP). OTAA involves the end-node sending a join request to the server with its DevEUI, AppEUI, and AppKey. In response, the server provides the sensor's address (DevAddr), the network security key (NwkSKey), and the application security key (AppSKey) necessary for network participation. On the other hand, ABP does not require the negotiation phase for address allocation since the keys (DevEUI, AppEUI, and AppKey) are pre-coded within the end-node itself. However, it is noted that ABP is considered less secure compared to the OTAA method due to its inherent design.

5.4 Experimental Set-Up & Results:

The layered architecture designed for the specific marine application consists of (1) end-nodes, embedded systems, and electronics dedicated to collecting and processing information and supporting communication; (2) multiple gateways responsible for data handling, message routing, and platform communication management; (3) a server whose duty is data aggregation; and (4) a web application that provides services to end-users.

In the field tests, various types of end-nodes were employed: commercially available sensors such as the Adeunis Field Test and the Dragino LT I/O Controller, alongside purpose-developed nodes. The latter category comprises three nodes TIAMO 1, TIAMO 2 engineered using an STM32L4X family ST microcontroller and a spectrometric sensor (referred to as a spectrometer) [33, 34].

These TIAMO end-nodes, depicted in Figure(a), were crafted utilizing STMicroelectronics STM32CubeMXW in software for low-level management and Atollic True STUDIO STM32 for high-level programming. The firmware generation involves defining the hardware through STM32CubeMX, which generates low-level code imported into Atollic True STUDIO. This setup enables the development of the board's operational logic using high-level programming languages like C and C++.

Additionally, these end-nodes were outfitted with compact meteorological sensors to capture temperature, humidity, and atmospheric pressure data.

On the other hand, the spectrometer (depicted in Figure (b)) was designed with an STS-VIS spectrometer by Ocean Insight, functioning in the visible range (350–800 nm). It's capable of estimating chlorophyll-a concentration and suspended sediment levels within medium-low concentration ranges. The processing unit consisted of a Raspberry Pi 3B equipped with a Sony IMX219 8-megapixel CMOS sensor capable of producing static images up to 3280 x

2464 pixels and supporting various video formats. The complete spectrometer setup also included a Dragino SX127X GPS HAT board an expansion module for the Raspberry Pi housing the Semtech SX1276/1278 transceiver and the Quectel L80-M39 GPS receiver. This board interfaces via the GPIO connector and operates directly from the Raspberry Pi's power supply.

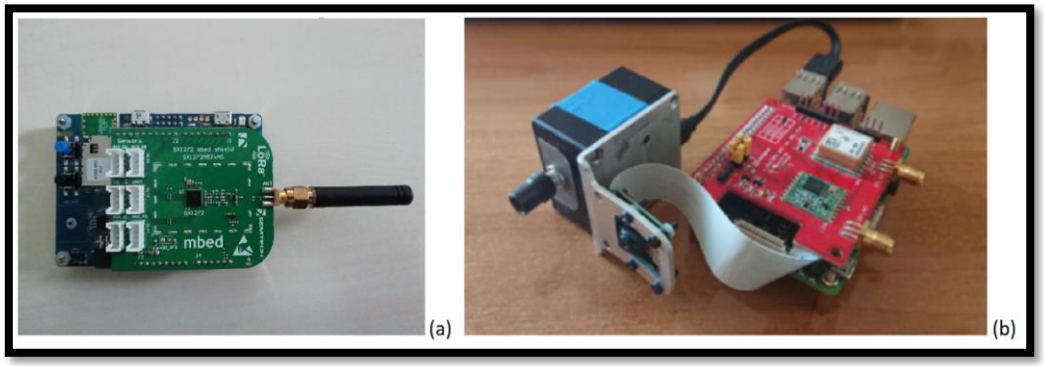

Figure 27: (A)The LoRaWAN end-node TIAMO developed for the acquisition of meteorological parameters. and (B) The spectrometer with the camera and the processing unit.

Five LG308 gateways by Dragino, each equipped with GPS and GSM capabilities, were utilized to transmit packets via Ethernet to a dedicated private LoRaWAN server. This server was linked to a backend component responsible for data processing, storage, and facilitated monitoring and analysis through an information system. The setup specifically involved configuring the open-source Chirp stack LoRaWAN Network server and employing the Swagger open-source project as the backend.

A web service was developed to visualize real-time vessel tracks fitted with IoT end-nodes. This served as a control center, detecting vessel presence within defined coastal areas, particularly those associated with protected marine zones. Additionally, a data dashboard was created for real-time visualization of marine environmental data, offering insights into the state of sea waters. Through-out the research, the LoRaWAN protocol optimized for data rates

was employed. All end-nodes were configured to register using OTAA, and detailed transmission parameters from the gateways used were logged.

Each node had a distinct payload size: the TIAMO nodes had a payload length of 12 bytes, the Field Test ranged from 8 to 24 bytes based on GPS data presence and push-button triggering, the LT I/O Controllers had a fixed payload size of 12 bytes, and the spectrometer maintained a payload size of 21 bytes.

The evaluation of LoRa connectivity occurred in two scenarios: the first in the coastal area near the Genova harbor and the second in the Northwestern Mediterranean Sea, characterized by steep coastal mountains. These geographical constraints enabled investigation of connectivity from open ocean to coast, leveraging the possibility of installing gateways on hill-sides behind the sea within line of sight (LOS) and adhering to Fresnel zone limitations.

Figure 28: (**a**) Map of the track of the passenger vessel travelling from Porto Antico to Pegli and of the position of the five gateways simultaneously operating on land, on hills behind the city center of Genoa. (**b**) Two TIAMO end-nodes for the acquisition of meteorological parameters, (**c**) Two LTI/O Controllers, and (**d**) The spectrometer installed on the passenger vessel.

All available land gateways were operational from 12:40 UTC to 15:40 UTC (Table 6), with the two passages from Porto Antico to Pegli and back departing at 13:25 UTC from Porto Antico and 13:50 UTC from Pegli, respectively.

Table 6: Position of the gateways used for tracking the passenger vessel.

Gateway Id	Position Id	Latitude	Longitude	Altitude
LG308 1	Crevari	44.42456	8.73098	169
LG308 2	Mount Gazzo	44.44229	8.84801	418
LG308 3	Mount Fasce	44.40790	9.01618	541
LG308 4	Righi	44.42564	8.93563	290
LG308 5	Scarpino	44.44416	8.86392	395

The second research took place aboard the R/V Dallaporta during the research cruise ICOS20 from October 19 to October 21, conducted by the National Research Council (CNR) of Italy. Departing and concluding in La Spezia, the three-day navigation route was determined by the requirements for conducting standard oceanographic measurements. These included tasks such as Conductivity Temperature Depth (CTD) casts and water sampling using the on-board rosette. The route encompassed the basin and the vicinity of the W1M3A observatory [35-37], an enduring infrastructure managed by the National Research Council (CNR) of Italy. This observatory is part of ERIC EMSO and constitutes the marine segment of ERIC ICOS, as illustrated in Figure 29.

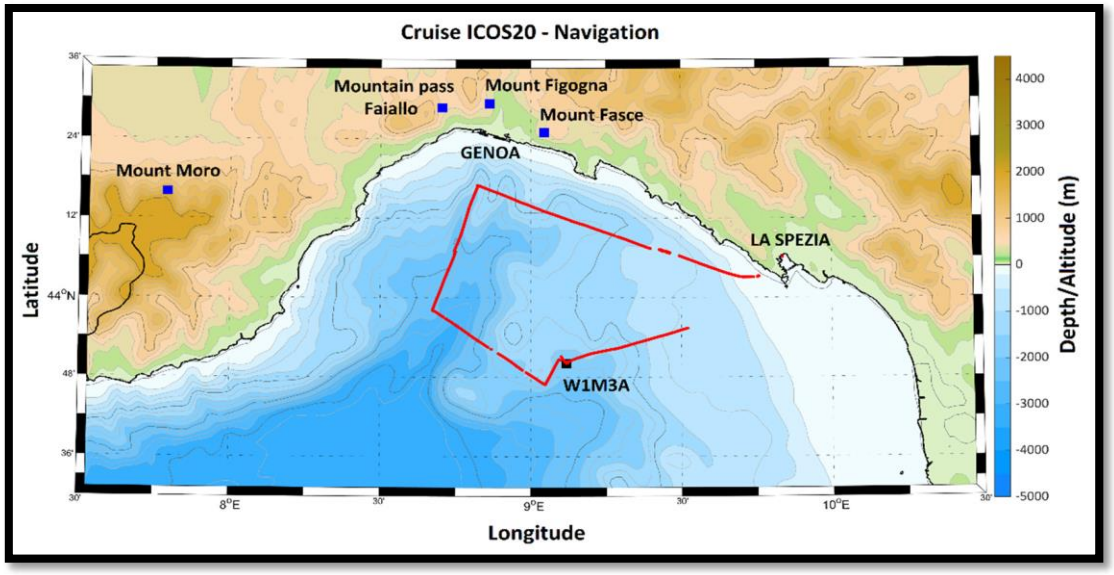

Figure 29: Depicts the operational area of the research cruise ICOS20, showcasing the positions of various elements: the gateways marked in blue squares, the W1M3A observatory denoted by a black square, and the track of the R/V Dallaporta highlighted in a red line.

Throughout the navigation, the end-node TIAMO 3 and an LT I/O Controller remained installed on the bow of the R/V Dallaporta. Meanwhile, the Field Test end-node was primarily positioned on the vessel's bow but was temporarily relocated to the W1M3A observatory during an inspection on the late afternoon.

Onboard the vessel, the gateway LG308 3 was placed in proximity to the nodes but transmitted LoRaWAN packets to the server solely when under GSM coverage.

Additionally, three gateways were operational along the coast on the evening of October 19 and the morning, serving to assess connectivity from open ocean to coast. Two LG308 gateways were positioned on hills behind Genoa, while another wireless gateway, managed by ISILINE s.r.l, operated on Mount Moro throughout the tests. One of the gateways, LG308 1, changed its location over the course of the two days. Table 7 provides a summary of the locations of these three gateways during the testing period**.**

Table 7: Positions of the gateways used during the research cruise on R/V Dallaporta.

Gateway ID	Day	Position ID	Latitude	Longitude	Altitude
LG308 1	19 October	Mountain-Faiallo	44.47830	8.70544	768
LG308 1	20 October	Mount Figogna	44.48920	8.86234	788
LG308 3	19 October	Mount Fasce	44.41759	9.04482	740
LG308 3	20 October	Mount Fasce	44.41702	9.04417	748
RAK	19 October	Mount Moro	44.26660	7.79067	17221
RAK	20 October	Mount Moro	44.26660	7.79067	17221

To evaluate the transmission performance, several metrics were taken into account:

1. Packet loss ratio

2. Packet reception rate (PRR)

3. Expected Signal Power (ESP)

4. Received Signal Strength Indication (RSSI)

5. Signal-to-Noise Ratio (SNR)

a) Received Signal Strength Indication (RSSI):

The RSSI, short for Received Signal Strength Indicator, measures the power of a received signal in milliwatts (dBm), indicating how well a receiver can detect a signal transmitted by a sender.

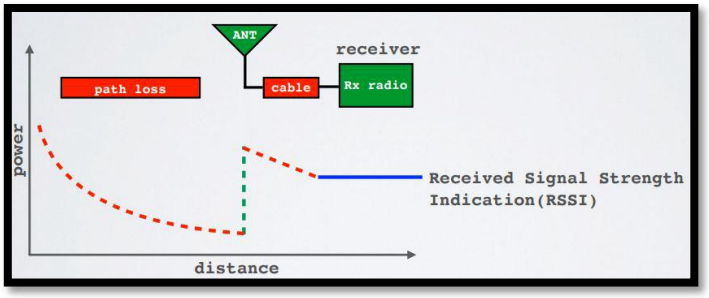

The RSSI unit is dBm and it is a negative value. RSSI value close to zero shows better signal strength. Typical LoRa RSSI values are:

RSSI minimum = -120 dBm.

If RSSI= -30 dBm: signal is strong.

If RSSI= -120 dBm: signal is weak.

b) Signal-to-Noise Ratio (SNR):

Signal-to-Noise Ratio (SNR) [71] is the ratio between received signal power and the noise power level. The noise floor is a region that contains all undesired interfering signal sources that might distort the transmitted signal and cause re-transmissions. Normally, the physical limit of sensitivity is the noise floor.

These metrics were derived or measured from the data available from the gateways. The packet loss ratio, ESP, and PRR were calculated using the following equations:

$$Packet\ Loss\ ratio = 1 - \frac{Number\ of\ packets\ recieved}{Number\ of\ packets\ sent}$$

$$ESP = RSSI + SNR - 10.log_{10}(1 + 10^{0.1\,SNR})$$

$$log_{10}(PRR) = PL.log_{10}(1 - BER) + log_{10}(P_S)$$

(5.9)

In these calculations, [37] BER represents the bit error rate, while Ps stands for the probability of successful preamble reception. The Ps term takes into account that the channel does not exhibit constant additive white Gaussian noise characteristics but behaves like a slow fading Rayleigh channel. Its calculation is derived from.

The BER is computed according to the proposed equations:

$$BER = Q\left(2.\frac{log_{12}(SF)}{\sqrt{2}}.\frac{E_b}{N_o}.\left(\frac{4}{4+CR}\right)\right)$$

$$\frac{E_B}{N_o} = SNR + 10.log_{10}\left(\frac{BW}{R_b}\right)$$

$$R_b = SF.\frac{BW}{2^{SF}}.\left(\frac{4}{4+CR}\right)$$

(5.10)

5.4.1 Results:

During the tests, all end-nodes functioned with a bandwidth of 125 kHz and a coding rate of 4/5. When the scale factor was adjusted from 6 to 12, the transmission speeds ranged from 5.48 kbit s^ {-1} to 0.30 kbit s^ {-1}. This demonstrates an inverse correlation between transmission speed and scale factor.

Throughout all tests, the Adaptive Data Rate algorithm was employed to optimize communication efficiency by minimizing energy consumption of the end-nodes. The sampling periods were standardized at 30 seconds for the LT I/O Controllers and Field Test, 60 seconds for the TIAMO end-nodes, and 20 seconds for the spectrometer.

When gateways and end-nodes are located close together, having a high link budget is not crucial because the time it takes for the transmitted packet to reach its destination is reduced. However, for longer distances such as in wide-area marine applications, a high link budget is essential. In this research, transmissions were carried out in the maximum

sensitivity scenario, which resulted in the highest packet loss due to a time-of-flight ranging from 1.2 to 1.9 seconds. The nominal frequency band used was 868 MHz.

During two tests on a passenger vessel, the developed LoRaWAN was tested for performance in both line of sight (LOS) and non-line of sight (NLOS) scenarios. As the vessel departed from Porto Antico, gateways at Righi, Mount Fasce, and partially at Mount Gazzo, Scarpino, and Crevari were the only ones with assured LOS. On the return trip from Pegli, all gateways were in LOS except for Righi.

Figure 30: LoraWAN Gateway Locations

The results of the test conducted in coastal waters and R/V Dallaporta showed varying packet loss ratio for each pair of end-node and gateway. The total number of packets transmitted by the Field Test end-node was 190, with the spectrometer sending 102 packets, LT I/O Controller 1 sending 45 packets, and end-node TIAMO 3 sending 71 packets. LT I/O Controller 2 was not operational due to a battery fault. In Pegli, the sea conditions prevented the spectrometer from operating, resulting in a high packet loss ratio for this end-node with the gateways at Crevari and Scarpino, despite being in LOS condition.

LT I/O Controller 1 only operated during the return journey from Pegli to Porto Antico, leading to a higher number of missed packets for LG308 1, which had partially obstructed line of sight (LOS) during the vessel's return to Porto Antico.

The most successful transmissions were observed in LOS conditions, regardless of the distance between the end-nodes and the gateways. This indicates that reliable transmissions can be achieved over vast stretches of sea, even when near the coast, by utilizing gateways in elevated positions with unobstructed views of the marine area of interest.

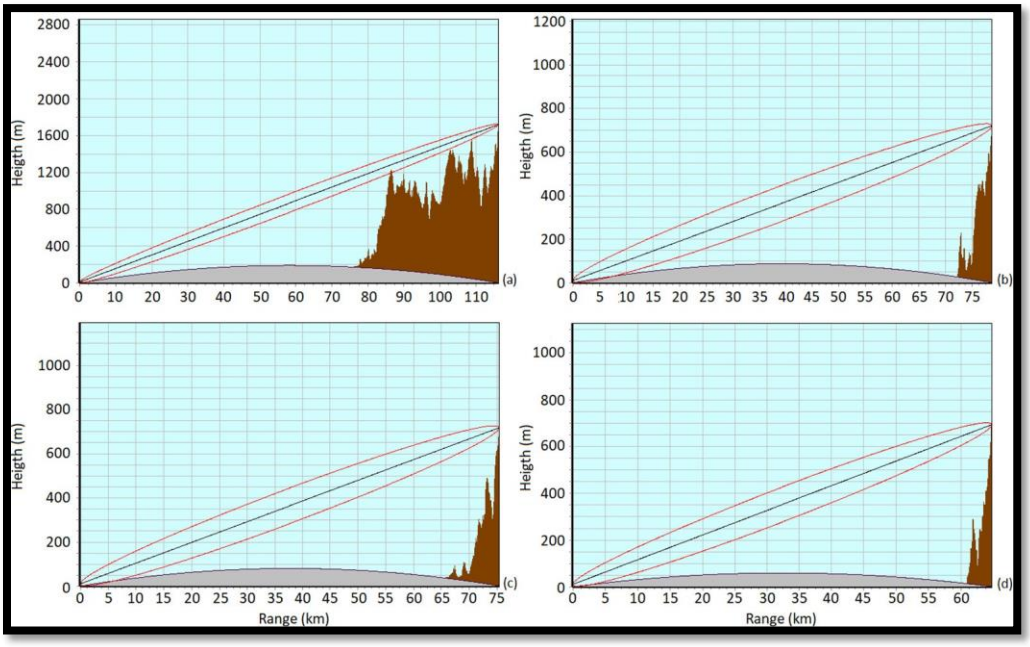

Figure 31: Gateway received the signals transmitted from the W1M3A observatory: (a) Mount Moro; (b) Mountain pass Faiallo; (c) Mount Figogna; (d) Mount Fasce. Grey areas show the curvature of the Earth. Ellipses correspond to the eight of the first Fresnel zone at 868 MHz. The Los is black line.

[Figure:31] The research findings demonstrate the possibility of obtaining reliable IoT transmission with end-nodes deployed on mobile platforms at sea, both close to the coast and in offshore settings. Successful transmissions were achieved over distances exceeding 100 km in unobstructed line of sight conditions, showcasing the high sensitivity of LoRa transmission up to 140 dBm in real-world maritime environments. Importantly, commercial end-nodes like Field Test and LT I/O Controller 1 performed similarly to the custom-developed TIAMO 3 end-node in terms of range capabilities.

The estimates of received power calculated using the Friis and Hata models (Equations 5.3-5.6) in a coastal setting, where gateways are placed on nearby hills and end-nodes are located on a passenger vessel, tend to slightly overstate the actual received power as determined by RSSI and SNR using Equation 5.9.

Table 8: Maximum achieved distance among nodes and gateways.

Gateway ID	Position ID	Latitude	Latitude	Maximum Distance Between gateway And End-Nodes (KM)
LG308 1	Mountain Faiallo	44.47830	8.70544	78.29
LG308 3	Mount fasce	44.41759	9.04482	71
RAK	Mount Moro	44.26660	7.79067	113
RAK	Forte Begato	64.26660	9.79067	140(On going)

The research results indicate that a distance of more than 110 km between gateways and end-nodes is possible in a marine environment under line-of-sight (LOS) conditions. The maximum distance achieved was 113 km, but it may not be the definitive limit for reliable LoRa transmission over water. This is due to the fact that the lowest detectable received power for LoRa transmission is -140 dB, while in the test it was measured at approximately -129 dB.

CONCLUSIONS

This study aimed to demonstrate the effectiveness of LoRa technology in a challenging marine environments setting by determining the maximum distance at which packets were successfully received by the gateway.

Thesis defined a detailed description of different Low Power Wide Area (LoRaWAN) technologies which are so famous these days due to some precious characteristics that are inevitable in the 4th industrial era. Furthermore, some comparisons between LoRa and LoRaWAN technologies along with the transmission parameters of LoRa and their selection in order to have a good communication performance on LoRa link have been outlined. In the end, we have set up a LoRaWAN network that includes a sensor node, a gateway and, a network server in order to build a communication based on Lora modulation to send packets toward the gateway.

The goal of the project was to design adaptive meshed sensor networks with a layered architecture based on the Internet of Things (IoT) concept for marine environments. These networks are able to communicate and adapt to changing conditions. An IoT network was created with end-nodes to monitor water quality and environmental parameters at sea, along with gateways, network, and application servers. The network was tested at sea under both Line of Sight (LOS) and Non-Line of Sight (NLOS) conditions using a passenger vessel in Genoa harbor and the R/V Dallaporta during an oceanographic cruise in Last October.

The research demonstrated the ability of a LoRaWAN protocol to transmit data over long distances (80-110 km) in LOS conditions, and buildings on data transmission in coastal scenarios. The result was promising, showing that compact, low-power, and easily manageable IoT sensors could be deployed on existing marine infrastructure networks, Research still Ongoing with extend kms. This technology could help authorities monitor

leisure boats in protected marine areas and provide them safety information. The Research estimated that several tens of end-nodes would be needed, which is feasible with a LoRaWAN network with multiple gateways.

While the tests were limited by European duty-cycle rules and the availability of ship time, the project demonstrated the potential for autonomous IoT sensors to improve monitoring and data collection in marine environments.

BIBLIOGRAPHY

1. LPWA network technologies and low-power standards. (n.d.). Retrieved June 21, 2021, from I-SCOOP: https://www.i-scoop.eu/internet-of-things-iot/lpwan/

2. Nitin Naik. (n.d.). LPWAN Technologies for IoT Systems: Ultra Narrow Band and Spread Spectrum. LPWAN Technologies for IoT Systems: Choice Between Ultra Narrow Band and Spread Spectrum, 8. Retrieved from LPWAN_IoT_UNB_SS_Naik.pdf.

3. A. Tolio, D. Boem, T. Marchioro, and L. Badia, "Spreading factor allocation in LoRa networks through a game theoretic approach," In Proc. IEEE International Conference on Communications (ICC), 2020.

4. Comtechefdata.com. (2012) Spread Spectrum in the SLM5650A: Features, performance, and applications. [Online]. Available: http://www.comtechefdata.com/files/articles papers/WPSpread-Spectrum-in-SLM-5650A.pdf

5. G. Kilian et al., "Increasing Transmission Reliability for Telemetry Systems Using Telegram Splitting," in IEEE Transactions on Communications, vol. 63, no. 3, pp. 949-961, March 2015, Doi: 10.1109/TCOMM.2014.2386859.

6. Á.F. Gambin, E. Gindullina, L. Badia, and M. Rossi, "Energy cooperation for sustainable IoT services within smart cities," In Proc. IEEE Wireless Communications and Networking Conference (WCNC), 2018.

7. Milarokostas, Christos; Tsolkas, Dimitris; Passas, Nikos; Merakos, Lazaros (2021): A Comprehensive Study on LPWANs with a Focus on the Potential of LoRa/LoRaWAN Systems. TechRxiv. Preprint. https://doi.org/10.36227/techrxiv.16853893.v1

8. Ertürk, M.A., Aydin, M.A., Buyukakkaslar, M.T., & Evirgen, H. (2019). A Survey on LoRaWAN Architecture, Protocol and Technologies. Future Internet, 11, 216.

9. Mekki, Kais & Bajic, Eddy & Chaxel, Frédéric & Meyer, Fernand. (2019). A comparative study of LPWAN technologies for large-scale IoT deployment. 5. 1-7. 10.1016/j.icte.2017.12.005.

10. A. Augustin, J. Yi, T. Clausen, and W. M. Townsley, "A Study of LoRa: Long Range & Low Power Networks for the Internet of Things," MDPI Sensor Journal, 2016.

11. V. Suryani., A. Rakhmatsyah., R. Y. Hasjim, "implementation wireless sensor network of IEEE 802.15.4 on human body temperature monitoring system," in international conference

on Innovative Engineering Technologies (ICIET2014), Bangkok, Thailand, 2014.

12. E. D. Ayele, C. Hakkenberg, J. P. Meijers, K. Zhang, N. Meratnia and P. J. M. Havinga, "Performance analysis of LoRa radio for an indoor IoT applications," in International Conference on Internet of Things for the Global Community (IoTGC), Fun- chal, Portugal, 2017.

13. de Carvalho Silva J., Rodrigues J.J.P.C., Alberti A.M., Solic P. & Aquino A.L.L. (2017) Lorawan A low power WAN protocol for Internet of Things: A review and opportunities. In: 2017 2nd International Multidisciplinary Conference on Computer and Energy Science (SpliTech), pp. 16.

14. Lennart Nordin. *LoRaWAN Device Classes: A, B and C*. 2018 (cit. on pp. 17–19).

15. A 1200.22 LoRaTM Modulation Basics, Rev. 2. Semtech, 2015, (accessed on17.09.2019).

16. Simtech. An In-depth look at LoRaWAN® Class A Devices (cit. on p. 16).

17. Simtech. What are LoRa® and LoRaWAN®? (Cit. on pp. 9, 15).

18. LoRa-Alliance, "Lorawan 1.1 specification," *technical specification*, 2017 https: //lora-alliance.org/resource-hub/lorawanr-specification-v11, Accessed: Oct.22,2020.

19. LoRa™ Alliance. «LoRaWAN™Regional Parameters v1.1rA». In: LoRaWAN™ 1.1 Specif. (2017) (cit. on pp. 4, 13).

20. Semtech. LoRa Modulation Basics AN1200.22. 2015 (cit. on p. 13).

21. "LoRa Overview cayenne docs." https://developers.mydevices.com/cayenne/docs/ lora/#lora. Accessed: Oct. 22, 2020.

22. A. Munari and L. Badia, "The role of feedback in AoI optimization under limited transmission opportunities," In Proc. IEEE GLOBECOM, pp. 1972-1977, 2022.

23. R. Wenner, "LoRa CHIRP Spread Spectrum lora chirp." https://www.youtube.com/ watch=dxYY097QNs0. Accessed: Oct. 24, 2020.

24. A. Tolio, D. Boem, T. Marchioro, and L. Badia, "A Bayesian game framework for a semi-supervised allocation of the spreading factors in LoRa networks, Proc. IEEE Annual Ubiquitous Computing, Electronics & Mobile Communication Conference (UEMCON) (pp. 0434-0439), 2020.

25. M. Knight, "Decoding LoRa exploring next-generation wireless networks."

https://github.com/matt-knight/research/tree/master/2016_12_29_ccc-33c3. accessed: Oct. 27, 2020.

26. Qoitech, "How Spreading Factor affects LoRaWAN device battery life the things conference partner." https://www.thethingsnetwork.org/article/ how-spreading-factor-affects-lorawan-device-battery-life. Accessed: Oct. 28, 2020.

27. ETSI, "Etsi tr 103 526: Technical characteristics for low power wide area networks chirp spread spectrum (lpwan-css)," *ETSI Technical Report*, 2018.

28. "Federal Communications Commission what we do." https://www.fcc.gov/about-fcc/ what-we-do, Jul 2017. Accessed: Feb. 20, 2020.

29. LoRa-Alliance, "Rp002-1.0.0 lorawan regional parameters," *Regional Parameters*, 2010. https://https://lora-alliance.org/sites/default/files/2019

30. Semtech-Corporation, "Lora and lorawan: A technical overview," *Technical Paper*, 2019.

31. Khalifeh, A.; Aldahdouh, K.A.; Darabkh, K.A.; Al-Sit, W. A Survey of 5G Emerging Wireless Technologies Featuring LoRaWAN, Sigfox, NB-IoT and LTE-M. In Proceedings of the 2019 International Conference on Wireless Communications Signal Processing and Networking (WiSPNET), Chennai, India, 21–23 March 2019; pp. 561–566.

32. Rappaport, T.S. *Wireless Communications: Principles and Practice*, 2nd ed.; Prentice Hall Communications Engineering and Emerging Technologies Series; Prentice Hall PTR: Upper Saddle River, NJ, USA, 2002; ISBN 978-0-13-042232-3.

33. Saelens, M.; Hoebeke, J.; Shahid, A.; Poorter, E.D. Impact of EU Duty Cycle and Transmission Power Limitations for Sub-GHz LPWAN SRDs: An Overview and Future Challenges. *J. Wireless Com. Netw.* 2019, *2019*, 219.

34. Moser, G.; De Martino, M.; Serpico, S.B. Estimation of Air Surface Temperature from Remote Sensing Images and Pixelwise Modeling of the Estimation Uncertainty Through Support Vector Machines. *IEEE J. Sel. Top. Appl. Earth Obs. Remote Sens.* 2015, *8*, 332–349.

35. Moser, G.; Zerubia, J. *Mathematical Models for Remote Sensing Image Processing*; Signals and Communication Technology; Moser, G., Zerubia, J., Eds.; Springer International Publishing: Cham, Switzerland, 2018; ISBN 978-3-319-66328-9.

36. Picco, P.; Bozzano, R.; Schiano, M.E.; Bordone, A.; Borghini, M.; Di Nallo, G.; Pensieri, S.; Schirone, A.; Sparnocchia, S. Marine Observing Systems from Fixed

Platform in the Ligurian Sea. *Bollettino Geofisica Teorica Applicata* 2007, *48*, 227–239.

37. Bozzano, R.; Pensieri, S.; Pensieri, L.; Cardin, V.; Brunetti, F.; Bensi, M.; Petihakis, G.; Tsagaraki, T.M.; Ntoumas, M.; Podaras, D.; et al. The M3A network of open ocean observatories in the Mediterranean Sea. In Proceedings of the 2013 MTS/IEEE OCEANS—Bergen, Bergen, Norway, 10–14 June 2013; pp. 1–10.

38. Canepa, E.; Pensieri, S.; Bozzano, R.; Faimali, M.; Traverso, P.; Cavaleri, L. The ODAS Italia 1 Buoy: More than Forty Years of Activity in the Ligurian Sea. *Prog. Oceanogr.* 2015, *135*, 48–63.

39. Attia, T.; Heusse, M.; Tourancheau, B.; Duda, A. Experimental characterization of LoRaWAN link quality. In Proceedings of the 2019 IEEE Global Communications Conference (GLOBECOM), Waikoloa, HI, USA, 9–13 December 2019; pp. 1–6.

40. M. A. Ahmed, J. L. Gallardo, M. D. Zuniga et al., "LoRa based IoT platform for remote monitoring of large-scale agriculture farms in Chile," *Sensors*, vol. 22, no. 8, p. 2824, 2022.

41. A. Marahatta, Y. Rajbhandari, A. Shrestha et al., "Evaluation of a LoRa mesh network for smart metering in rural locations," *Electronics*, vol. 10, no. 6, p. 751, 2021.

42. M. Pan, C. Chen, X. Yin, and Z. Huang, "UAV-aided emergency environmental monitoring in infrastructure-less areas: LoRa mesh networking approach," *IEEE Internet of Cings Journal*, vol. 9, no. 4, pp. 2918–2932, 2022.

43. N. A. Alam, M. Ahsan, M. A. Based, J. Haider, and E. M. G. Rodrigues, "Smart monitoring and controlling of appliances using lora based iot system," *Design*, vol. 5, 2021.

44. A. Zancanaro, G. Cisotto, and L. Badia, "Tackling Age of Information in Access Policies for Sensing Ecosystems," Sensors, 23(7), p.3456, 2023.

45. R. K. Singh, M. Aernouts, M. De Meyer, M. Weyn, and R. Berkvens, "Leveraging LoRaWAN technology for precision, agriculture in greenhouses," *Sensors*, vol. 20, no.

46. L. Parri, S. Parrino, G. Peruzzi, and A. Pozzebon, "A LoRaWAN network infrastructure for the remote monitoring of onshore sea farms," in *Proceedings of the 2020 IEEE International Instrumentation and Measurement Technology Conference (I2MTC)*, pp.

47. A. D. Boursianis, M. S. Papadopoulou, A. Gotsis et al., "Smart irrigation system for precision agriculture – the ARE-OU5A IoT platform," *IEEE Sensors Journal*, vol. 21, no.16,Article,ID,17539,2021.

48. G. Codeluppi, A. Cilfone, L. Davoli, and G. Ferrari, "LoraFarM: a LoRaWAN-based smart farming modular IoT architecture," *Sensors*, vol. 20, no. 7, p. 2028, 2020.

49. A. Valente, S. Silva, D. Duarte, F. Cabral Pinto, and S. Soares, "Low-cost lorawan node for agro-intelligence iot," *Electronics*, vol. 9, no. 6, pp. 987–1017, 2020.

50. C. Kamienski, J. P. Soininen, M. Taumberger et al., "Smart water management platform: IoT-based precision irrigation for agriculture," *Sensors*, vol. 19, no. 2, p. 276, 2019.

51. P. A. Catherwood, D. Steele, M. Little, S. McComb, and J. McLaughlin, "A community based IoT personalized wireless healthcare solution trial," *IEEE Journal of Translational Engineering in Health and Medicine*, vol. 6, pp. 1–13, 2018.

52. A. T. Nugraha, R. Wibowo, M. Suryanegara, and N. Hayati, "An IoT-LoRa system for tracking a patient with a mental disorder: correlation between battery capacity and speed of movement," in *Proceedings of the 2018 7th International Conference on Computer and Communication Engineering (ICCCE)*, pp. 198–201, Kuala Lumpur, Malaysia, September 2018.

53. R. Susanto and J. Anthony, "Comparison of three LoRa devices and its application on street light monitoring system," *IOP Conference Series: Earth and Environmental Science*,vol.195,Article,ID,012066,2018.

54. M. F. Tsai, Y. C. Kiong, and A. Sinn, "Smart service relying on Internet of -ings technology in parking systems," *Ce Journal of Supercomputing*, vol. 74, no. 9, pp. 4315–4338,2018.

55. Polonelli, T.; Brunelli, D.; Benini, L. Slotted ALOHA Overlay on LoRaWAN: A Distributed Synchronization Approach. In Proceedings of the 16th IEEE International Conference on Embedded and Ubiquitous Computing (EUC 2018), Bucharest, Romania, 24–26 October 2018; pp. 1–7.

56. Reynders, B.; Wang, Q.; Tuset-Peiro, P.; Vilajosana, X.; Pollin, S. Improving Reliability and Scalability of LoRaWANs Through Lightweight Scheduling. IEEE Internet Things J.2018,5,1830–1842.

57. Almeida, R.; Oliveira, R.; Luís, M.; Senna, C.; Sargento, S. A Multi-Technology Communication Platform for Urban Mobile Sensing. Sensors 2018, 18, 1184.

58. Haxhibeqiri, J.; Moerman, I.; Hoebeke, J. Low Overhead Scheduling of LoRa Transmissions for Improved Scalability. IEEE Internet Things J. 2018.

59. LoRa Alliance. LoRaWAN Specifications v1.0; LoRa Alliance: Fremont, CA, USA, 2015.

60. LoRa Alliance. LoRaWAN Specifications v1.1; LoRa Alliance: Fremont, CA, USA, 2017.

61. Duda, A.; To, T.H. Simulation of LoRa in NS-3: Improving LoRa Performance with CSMA. In Proceedings of the IEEE ICC, Kansas City, MO, USA, 20–24 May 2018.

62. Kouvelas, N.; Rao, V.; Prasad, R. Employing p-CSMA on a LoRa Network Simulator. 2018,arXiv:1805.12263.

63. Almeida, R.; Oliveira, R.; Sousa, D.; Luis, M.; Senna, C.; Sargento, S. A Multi-Technology Opportunistic Platform for Environmental Data Gathering on Smart Cities. In Proceedings of the 2017 IEEE Globecom Workshops (GC Wkshps), Singapore, 4–8 December,2017;pp.17.

64. Centenaro, M.; Vangelista, L. Boosting network capacity in LoRaWAN through time-power multiplexing. In Proceedings of the IEEE PIMRC, Bologna, Italy, 9–12 September,2018;pp.1–6.

65. G. Orestis and R. Usman, “Low Power Wide Area Network Analysis: Can LoRa Scale?”, in IEEE Wireless Communications Letters, vol. 6, IEEE, 2017, pp. 162–165.

66. https://publications.lib.chalmers.se/records/fulltext/252610/252610.pdf.

67. Visbeck, M. Ocean Science Research Is Key for a Sustainable Future. Nat. Commun. 2018,9,690.

68. Pinardi, N.; Stander, J.; Legler, D.M.; O’Brien, K.; Boyer, T.; Cuff, T.; Bahurel, P.; Belbeoch, M.; Belov, S.; Brunner, S.; et al. The Joint IOC (of UNESCO) and WMO Collaborative Effort for Met-Ocean Services. Front. Mar. Sci. 2019, 6, 410.

69. Smith, K., Jr.; Messié, M.; Sherman, A.; Huffard, C.; Hobson, B.; Ruhl, H.; Boetius, A. Navigating the Uncertain Future of Global Oceanic Time Series. Eos 2015, 96.

70. Weller, R.A.; Baker, D.J.; Glackin, M.M.; Roberts, S.J.; Schmitt, R.W.; Twigg, E.S.; Vimont, D.J. The Challenge of Sustaining Ocean Observations. Front. Mar. Sci. 2019,

71. Albaladejo, C.; Sánchez, P.; Iborra, A.; Soto, F.; López, J.A.; Torres, R. Wireless Sensor Networks for Oceanographic Monitoring: A Systematic Review. Sensors 2010, 10, 6948.

72. L. Badia, "Impact of transmission cost on age of information at Nash equilibrium in slotted ALOHA," IEEE Networking Letters, 4(1), 2021.

73. Andrews, J.G.; Ghosh, A.; Muhamed, R. Fundamentals of WiMAX: Understanding Broadband Wireless Networking; Prentice-Hall: Englewood Cliffs, NJ, USA, 2011; ISBN.978-0-13-290780-4.

74. Bekkadal, F.; Yang, K. Novel maritime communications technologies. In Proceedings of the 2010 10th Mediterranean Microwave Symposium, Guzelyurt, Northern Cyprus, 25–27 August 2010; IEEE: Guzelyurt, Turkey, 2010; pp. 338–341.

75. Vangelista, L.; Zanella, A.; Zorzi, M. Long-range IoT technologies: The dawn of LoRaTM. In Future Access Enablers for Ubiquitous and Intelligent Infrastructures; Lecture Notes of the Institute for Computer Sciences, Social Informatics and Telecommunications Engineering; Atanasovski, V., Leon-Garcia, A., Eds.; Springer International Publishing: Cham, Switzerland, 2015; Volume 159, pp. 51–58, ISBN 978-3-319-27071-5.

76. Bardyn, J.P.; Melly, T.; Seller, O.; Sornin, N. The Era of LPWAN Is Starting Now; IEEE: New York, NY, USA, 2016; pp. 25–30.

77. Xu, G.; Shi, Y.; Sun, X.; Shen, W. Internet of Things in Marine Environment Monitoring: A Review. Sensors 2019, 19, 1711.

78. Marcelli, M.; Piermattei, V.; Gerin, R.; Brunetti, F.; Pietrosemoli, E.; Addo, S.; Boudaya, L.; Coleman, R.; Nubi, O.A.; Jojannes, R.; et al. Toward the Widespread Application of Low-Cost Technologies in Coastal Ocean Observing (Internet of Things for the Ocean). Medit. Mar. Sci. 2021, 22, 255–269.

79. Li, L.; Ren, J.; Zhu, Q. On the application of LoRa LPWAN technology in sailing monitoring system. In Proceedings of the 2017 13th Annual Conference onWireless On-demand Network Systems and Services (WONS), Jackson, WY, USA, 21–24 February 2017;pp.77–80.

80. Parri, L.; Parrino, S.; Peruzzi, G.; Pozzebon, A. Low Power Wide Area Networks (LPWAN) at Sea: Performance Analysis of Offshore Data Transmission by Means of LoRaWAN Connectivity for Marine Monitoring Applications. Sensors 2019, 19, 3239.

81. Haxhibeqiri, J.; Van den Abeele, F.; Moerman, I.; Hoebeke, J. LoRa Scalability: A Simulation Model Based on Interference Measurements. Sensors 2017, 17, 1193.

82. Croce, D.; Gucciardo, M.; Mangione, S.; Santaromita, G.; Tinnirello, I. Impact of LoRa Imperfect Orthogonality: Analysis of Link-Level Performance. IEEE Commun. Lett. 2018,22,796–799.

83. Real Wireless. (2015) A comparison of UNB and spread spectrum wireless technologies as used in LPWA M2M applications. [Online]. Available: https://www.thethingsnetwork.org/forum/uploads/default/original/1X/3b1c1ae4a925e9aa897110ccde10ec61f3106b87.pdf.

84. F. Chiariotti and L. Badia, "Strategic Age of Information Aware Interaction Over a Relay Channel," IEEE Transactions on Communications, vol. 72, no. 1, pp. 101--116, Jan.2024.